2 Component reliability and system availability

One of the main potential advantages identified for microgrids is the possibility of achieving higher power supply availability as compared with conventional systems fed by a main electric grid. Thus, in order to quantitatively assess LAPES value and design constraints it is important to understand reliability and availability aspects of microgrids. Hence, the goal of this chapter is to define and discuss key attributes related to availability and reliability in LAPES.

2.1 Definitions

Consider first an entity – i.e., an item, such as a system component or a device. Reliability $R(t)$ of this entity is, then, defined as the probability that this item will operate under specified conditions without failure from some initial time $t = 0$ when it is placed into operation until a time t. The definition of failure of a component can take different forms. For some components, such as a resistor or a capacitor or most other passive circuit components or semiconductor devices, a failure implies that the component cannot operate meeting its intended function – e.g., a capacitor is experiencing a failure when it can no longer store electrical energy according to its given capacitance. For other components, such as batteries, a failure occurs when the component can no longer meet some performance requirements – e.g., a battery can be considered to have failed when at a given nominal temperature its capacity falls below a given percentage of its nominal capacity. That is, for the latter type of component, some level of performance degradation is accepted without implying a failure condition. Notice that one key aspect of the definition of reliability is that it is defined as a probability. Hence, it can only take values between 0 and 1. Another key aspect of this definition is that the entity needs to operate without failure during the entire period of time under evaluation. That is, the repairing concept is implicitly not considered as part of the evaluation of component reliability. The complementary concept to reliability is called unreliability $F(t)$. Hence, in a mathematical form it is

$$F = 1 - R \tag{2.1}$$

That is, unreliability is the probability that an item fails to work continuously over a stated time interval. The explicit statement in this definition that the item needs to work

https://doi.org/10.1017/CBO9781139002998.003 Published online by Cambridge University Press

continuously is related to the notion that the item should not experience any failure, as was mentioned in the definition of reliability. As a result of these notions, it is implicitly assumed that the concept of reliability cannot be applied directly to repairable components or systems.

For systems or repairable items, the concept that describes their behavior in terms of the possibility of being in a failed state or not is called availability. The term availability can be used in different senses, depending on the type of system or item under consideration [1]:

1. Availability, A, is the probability that an entity works on demand. This definition is adequate for standby systems.
2. Availability, $A(t)$ is the probability that an entity is working at a specific time t. This definition is adequate for continuously operating systems.
3. Availability, A, is the expected portion of the time that an entity performs its required function. This definition is adequate for repairable systems.

The last definition is the one among the three that represents best the differences between the definitions of reliability and availability. One of these differences was already pointed out and relates to the notion that reliability is a concept that does not apply to systems that may go out of service due to either unexpected or expected causes, and that are brought back to service after some time has passed. Another of the differences between the concepts of availability and reliability originates in the fact that many systems can maintain operation within required parameters even when some of their components are out of service, or, after a failure, when not all components that have failed have been repaired. As was done for the definition of reliability, it is possible to define a complement to availability; this complement is called unavailability U_a.

2.2 Basic theory and concepts

Once the concepts of reliability and availability are introduced, it is possible to explore in more detail their application and use. This is the focus of this section.

2.2.1 Reliability

Reliability of an item is, typically, evaluated based on its failure characteristics. That is, reliability is often calculated by evaluating unreliability first. Unreliability of an item can be evaluated from

$$F(t) = \Pr\{\text{a given item fails in } [0, t]\} \tag{2.2}$$

where Pr{event} represents the probability of occurrence of a given event. Notice that continuous operation is implicit in (2.2) and that $F(t)$ can be considered as a cumulative distribution function of a random variable t with a probability density function $f(t)$ given by

https://doi.org/10.1017/CBO9781139002998.003 Published online by Cambridge University Press

$$f(t) = \frac{dF(t)}{dt} \tag{2.3}$$

which implies that

$$f(t) \;=\; \Pr\{\text{a given item fails in } [t, t+dt]\} \tag{2.4}$$

and

$$F(t) = \int_0^{\tau} f(\tau)d\tau \tag{2.5}$$

Still, (2.3) to (2.5) do not provide a practical way of representing the reliability characteristics of a circuit component. Thus, a hazard function $h(t)$ is used in order to characterize an item's behavior in terms of transitioning from a working to a failed state. This function provides a more practical perspective for characterizing an entity's reliability behavior by representing the expected rate at which failures occur. Mathematically, $h(t)dt$ indicates the probability that an item fails between t and $t + dt$ given that it has not failed until t. That is, if the event A is "*an item fails between t and t + dt*" and event B is "*the same item has not failed until t*," then based on Bayes' theorem,

$$h(t)dt = \Pr\{A \mid B\} = \frac{\Pr\{B \mid A\}\Pr\{A\}}{\Pr\{B\}} = \frac{\Pr\{A\}}{\Pr\{B\}} \tag{2.6}$$

because $\Pr\{B|A\} = 1$. Now, from (2.4) $\Pr\{A\} = f(t)$, and from the combination of (2.1) and (2.2) $\Pr\{B\} = 1 - F(t)$. Hence,

$$h(t)dt = \frac{f(t)}{1 - F(t)} \tag{2.7}$$

Considering (2.5), if both sides of (2.7) are integrated along the interval 0 and t, then

$$F(t) = 1 - e^{-\int_0^t h(\tau)d\tau} \tag{2.8}$$

Although seemingly counterintuitive, (2.8) provides a practical way of knowing $F(t)$ from $h(t)$. In practical applications, $h(t)$ is relatively simple to evaluate when it is stipulated that $h(t)$ measures the anticipated number of failures of a given item during an specified time period. That is, the unit of measurement for $h(t)$ is 1/hour, 1/year, or any other equivalent unit. Evaluation of $h(t)$ leads to the well-known "bathtub curve" shown in Figure 2.1, which is obtained by counting the number of failures occurring during a given period for a large set of identical items that are placed into operation at the same time and that operate under the same conditions.

Notice in Figure 2.1 that during the useful life period of electronic components, their hazard function is constant. This constant value for $h(t)$ is conventionally named the constant failure rate λ. Hence, when $h(t)$ is replaced in (2.8) by this constant value λ, $F(t)$ becomes equal to

https://doi.org/10.1017/CBO9781139002998.003 Published online by Cambridge University Press

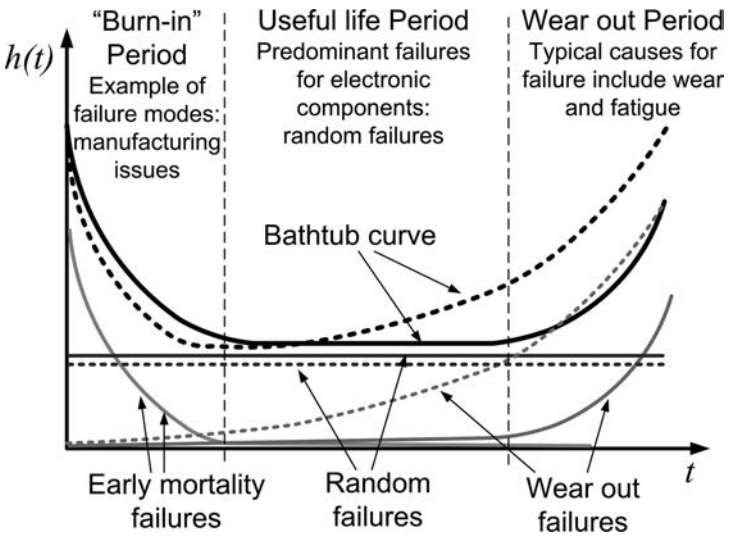

Figure 2.1 Typical bathtub curves and their components for electronic components (solid lines) and mechanical components (dotted lines). In practical applications the useful life period is much longer than the other periods.

$$F(t) = 1 - e^{-\lambda t} \tag{2.9}$$

Hence,

$$f(t) = \lambda e^{-\lambda t} \tag{2.10}$$

and

$$R(t) = e^{-\lambda t} \tag{2.11}$$

Thus, the reliability of an item with a constant failure rate is represented by an exponentially decaying function in which at time $t = 0$ there is no chance of observing a failure and in which there is almost a 37% chance of not observing a failure in the component from the time it was put into operation to the time given by $1/\lambda$. The value of $1/\lambda$ has another very important meaning in reliability theory: consider (2.10); the expected value for such a probability density function is

$$E[f(t)] = \int_0^\infty t f(t) dt = \frac{1}{\lambda} \tag{2.12}$$

which is denoted as the mean time to failure (MTTF) of the component under consideration.

2.2.2 Availability

Let's consider now an entity that can be repaired and brought back into operation when it fails. In this case, a failure rate $\lambda(t)$ can be used to represent the failure process of such a repairable entity. This failure rate is defined as

https://doi.org/10.1017/CBO9781139002998.003 Published online by Cambridge University Press

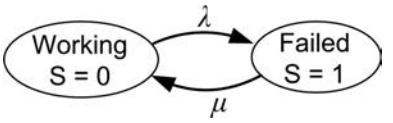

Figure 2.2 Markov process representing the operational state S of a single entity.

$$\lambda(t)dt = \frac{\Pr\{\text{item fails in } [t, t+dt]\}}{\Pr\{\text{item was working at } t = t\}} \tag{2.13}$$

which is analogous to (2.6) except for the different description of what was called event B in order to consider here the possibility that the item under evaluation has failed one or more times since it was first put into operation a long time in the past. In the same way, a repair rate $\mu(t)$ can be defined as

$$\mu(t)dt = \frac{\Pr\{\text{item is repaired in } [t, t+dt]\}}{\Pr\{\text{item was not working at } t = t\}} \tag{2.14}$$

in order to represent the random process involved with having the item transitioning from a failed state to a working state. If the state of the item (failed or operating normally) is considered to be independent of its past or future behavior – i.e., failures and repairs are independent of previous or future failures and repairs – the entity's behavior can be mathematically represented by a Markov process like the one graphically represented in Figure 2.2, with transition rates λ from the "working" state to the "failed" state and μ from the "failed" state to the "working" state. These transition rates are, in general, assumed to be at a constant rate.

In Figure 2.2, and based on (2.13) and (2.14), the probability that a repairable item will transition from the working state to the failed state is given by λdt, whereas the probability associated to the converse transition is μdt. Obviously, the probability of remaining in the working state is given by $(1-\lambda)dt$ and the probability of remaining in the failed state is $(1-\mu)dt$. Consider now the third definition of availability given in Section 2.1. It follows that the instantaneous unavailability of the discussed entity can be associated with the behavior of the item with respect to the failed state $S = 1$. That is, if the probability of finding the entity at the failed state of $t = t + dt$ is identified as $\Pr_f(t + dt)$, then this probability equals the probability that the item was working at time t and experienced a failure during the interval dt or that the item was already in the failed state at time t and it was not repaired during the immediately following interval dt. In mathematical terms

$$\Pr_f(t+dt) = \Pr_w(t)\lambda dt + \Pr_f(t)(1-\mu)dt \tag{2.15}$$

where $\Pr_w(t)$ is the probability that the item is at state $S = 0$ at time t. Thus,

$$\frac{\Pr_f(t+dt) - \Pr_f(t)}{dt} = \Pr_w(t)\lambda - \Pr_f(t)\mu \tag{2.16}$$

https://doi.org/10.1017/CBO9781139002998.003 Published online by Cambridge University Press

Since it is assumed that the time interval dt is infinitely small, the left side of (2.16) is, by definition, the time derivative of $\Pr_f(t)$. Moreover, $\Pr_f(t) = 1 - \Pr_w(t)$. Thus,

$$\frac{d\Pr_f(t)}{dt} = -(\lambda + \mu)\Pr_f(t) + \lambda \tag{2.17}$$

which is a first-order differential equation. If it is assumed that at time $t = 0$ the item is known to have been operating normally, then $\Pr_f(t = 0) = 0$, and the solution for (2.17) is

$$\Pr_f(t) = \frac{\lambda}{\lambda + \mu}\left(1 - e^{-(\lambda+\mu)t}\right) \tag{2.18}$$

which implies that

$$\Pr_w(t) = \frac{1}{\lambda + \mu}\left(\mu - \lambda e^{-(\lambda+\mu)t}\right) \tag{2.19}$$

Both (2.18) and (2.19) can be plotted, yielding the graph in Figure 2.3. The steady-state probabilities of finding the item under study in a failed or in a working state are also shown in this figure. These two probabilities represent how likely it is to have the entity under study operating normally or in a failed condition after placing the entity into operation for the first time a long time in the past. That is, these steady-state values indicate the availability and unavailability of the item under study:

$$A = \frac{\mu}{\lambda + \mu} \tag{2.20}$$

and

$$U_a = \frac{\lambda}{\lambda + \mu} \tag{2.21}$$

Equation (2.20) confirms that availability depends on two processes. One of those processes, the failure process, is (as is further discussed in Section 2.3) mostly related to an item's "hard" intrinsic and environmental conditions – such as operational temperature – whereas the other, the repair process, is also related to "soft" external factors – such as maintenance strategies, spare parts management, and logistical

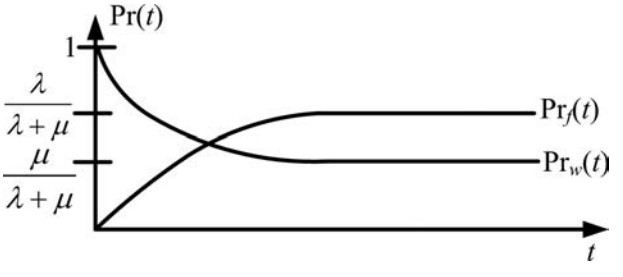

Figure 2.3 Example of typical time dependency associated with failed and working conditions of an entity.

https://doi.org/10.1017/CBO9781139002998.003 Published online by Cambridge University Press

processes. Clearly, the concept of reliability is embedded in that of availability. Hence, in the same way that the concept of MTTF was previously defined, it is possible now to define a mean up time (MUT) as the inverse of the failure rate λ and a mean downtime (MDT) as the inverse of the repair rate μ. The MDT includes the processes of detecting the failure, repairing the failure, and putting the item back into operation. The mean time between failures (MTBF) is defined as the sum of the MUT and MDT. With these definitions the availability and unavailability of an entity can be calculated based on

$$A = \frac{MUT}{MTBF} \tag{2.22}$$

and

$$U_a = \frac{MDT}{MTBF} \tag{2.23}$$

respectively.

2.2.3 Availability calculation techniques in systems

In Section 2.2.2 a Markov process was used to explore the availability behavior of a single item – i.e., a single component system. The same approach can be used for multicomponent systems. Consider, for example, a system with two components characterized by a Markov process with four states identified by S_1 to S_4, as shown in Figure 2.4. As this figure shows, a state can also be identified by a binary number in which the first digit represents the reliability condition of component A – the first digit is 0 if the component is in a state of normal operation and 1 if the component is in a failed situation – and the second digit represents the condition of component B. The differential equation that represents the behavior of the system is now given by

$$\left(\frac{d\mathbf{P}}{dt}\right)^T = \mathbf{P}^T\mathbf{A} \tag{2.24}$$

where the transition rates matrix $\mathbf{A}$ is

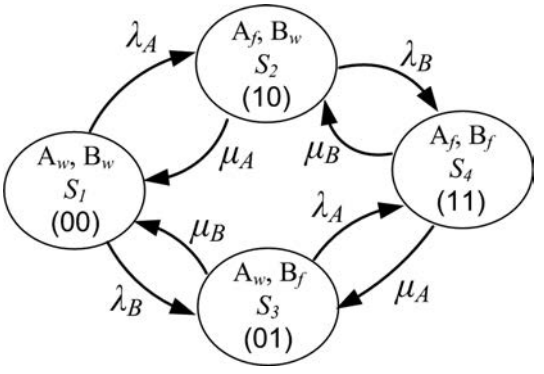

Figure 2.4 Markov process representation of the operational condition of a two-component system.

https://doi.org/10.1017/CBO9781139002998.003 Published online by Cambridge University Press

$$\mathbf{A} = \begin{pmatrix} -(\lambda_A + \lambda_B) & \lambda_A & \lambda_B & 0 \\ \mu_A & -(\mu_A + \lambda_B) & 0 & \lambda_B \\ \mu_B & 0 & -(\mu_B + \lambda_A) & \lambda_A \\ 0 & \mu_B & \mu_A & -(\mu_A + \mu_B) \end{pmatrix} \tag{2.25}$$

and where $\mathbf{P}^T$ is a transpose vector in which each coordinate is the probability of finding the system in each of the four states. That is,

$$\mathbf{P}^T = (\Pr_{S_1}(t) \quad \Pr_{S_2}(t) \quad \Pr_{S_3}(t) \quad \Pr_{S_4}(t)) \tag{2.26}$$

Equation (2.24) cannot be directly solved because **A** is singular. In order to solve it, it is necessary to consider the additional condition that the sum of all coordinates of **P** equals 1. When this condition and initial conditions are considered, it is usually possible to solve (2.24) with the added assumption that failure and repair rates are constant. Steady-state solutions can also be found from (2.24) by simply solving the algebraic system of equations that is obtained by making the left-hand side of (2.24) 0 and replacing one of the equations by the algebraic condition that the sum of all coordinates of **P** equals 1. The solutions for such a system of equations are shown in Table 2.1.

Table 2.1 also shows the expected time that the system remains in each of the states S_i and the frequency of finding the system in a given state. It has been shown in [1] that the expected time that the system remains in state S_i is given by

$$\bar{T}_i = \frac{1}{-a_{ii}} = \frac{1}{\sum_{\substack{j=1 \\ j \neq i}}^{N_s} a_{ij}} \tag{2.27}$$

where N_S is the total number of states in the Markov process representing the system under study and a_{ij} is the element in row i and column j of the matrix **A**. That is, the denominator in (2.27) is the negative of the diagonal element corresponding to the row and column of state S_i, which is minus the total rate of departure from S_i.

Table 2.1 Steady-state probabilities and relevant parameters for the four states in the Markov process representation of a two-component system.

State	$\Pr_{S_i}(t \to \infty)$	$\overline{T}_i$	ϕ_i
S_1	$\frac{\mu_A \mu_B}{(\mu_A + \lambda_A)(\mu_B + \lambda_B)}$	$\frac{1}{\lambda_A + \lambda_B}$	$\frac{\mu_A \mu_B (\lambda_A + \lambda_B)}{(\mu_A + \lambda_A)(\mu_B + \lambda_B)}$
S_2	$\frac{\lambda_A \mu_B}{(\mu_A + \lambda_A)(\mu_B + \lambda_B)}$	$\frac{1}{\mu_A + \lambda_B}$	$\frac{\lambda_A \mu_B (\mu_A + \lambda_B)}{(\mu_A + \lambda_A)(\mu_B + \lambda_B)}$
S_3	$\frac{\mu_A \lambda_B}{(\mu_A + \lambda_A)(\mu_B + \lambda_B)}$	$\frac{1}{\lambda_A + \mu_B}$	$\frac{\mu_A \lambda_B (\lambda_A + \mu_B)}{(\mu_A + \lambda_A)(\mu_B + \lambda_B)}$
S_4	$\frac{\lambda_A \lambda_B}{(\mu_A + \lambda_A)(\mu_B + \lambda_B)}$	$\frac{1}{\mu_A + \mu_B}$	$\frac{\lambda_A \lambda_B (\mu_A + \mu_B)}{(\mu_A + \lambda_A)(\mu_B + \lambda_B)}$

https://doi.org/10.1017/CBO9781139002998.003 Published online by Cambridge University Press

Equation (2.27) is obtained from knowing the probability density function of being at state S_i, which is [1]

$$f_{T_i}(T_i = \tau) = -a_{ii}e^{a_{ii}\tau} \tag{2.28}$$

Also from [1] it can be shown that the frequency of finding the system in state S_i is

$$\phi_i = -a_{ii}\Pr_{S_i}(t \to \infty) \tag{2.29}$$

Although the Markov process representation provides many insights into the availability behavior of a system, its application may become tedious as the number of components increases. One of the alternative methods to represent the availability behavior of a system is through "availability success diagrams." An availability success diagram is a graphic representation of the availability relationships among components in a system. Such a diagram has the following four parts:

1. A starting node
2. An ending node
3. A set of intermediate nodes
4. A set of edges

In the availability success diagram the edges represent the system components and the nodes represent the system structure from an availability standpoint. This structure may be different from a physical or an electrical topology. For example, if the system is an electrical circuit in which there are two components that are electrically connected in parallel but that are critical for the circuit operation – i.e., if one of those components fail, the system is in a failed state – then in an availability success diagram they are represented in a series connection. The expected system operating condition is represented with paths through the network. The system is in a working condition when all the components along at least one path from the starting node to the end node are operating normally. If there are enough failed components that it is not possible to find at least one path from the starting node to the end node with all the components operating normally, then the system is in a failed state.

Another method of representing and calculating system availability is the minimal cut sets (mcs) method. An mcs is a group of failed components that places the system in a failed state when all of its components are in a failed state – failure being characterized in a LAPES by the impossibility of the system completely supplying the load – but which returns the system to an operational state if any single one of its components is repaired. Once the mcs of a system are identified, the unavailability of a system can be calculated from

$$U_a = \Pr\left\{\bigcup_{j=1}^{M_C} K_j\right\} \tag{2.30}$$

where K_j represents the M_c mcs in the system. Calculating system unavailability using the exact expression in (2.30) is a very tedious process involving identifying the

https://doi.org/10.1017/CBO9781139002998.003 Published online by Cambridge University Press

probability of the logical union of many events. However, the calculation can be simplified by recognizing that U_a is bounded by

$$\sum_{i=1}^{M_c} \Pr\{K_i\} - \sum_{i=2}^{M_c} \sum_{j=1}^{i-1} \Pr\{K_i \cap K_j\} \leq U_a \leq \sum_{i=1}^{M_c} \Pr\{K_i\} \tag{2.31}$$

Thus, if all considered components are highly available, then U_a can be approximated to

$$U_a \cong \sum_{j=1}^{M_C} \Pr\{K_j\} \tag{2.32}$$

where $\Pr\{K_j\}$ is the probability of observing the mcs j happening. Such probability can be calculated based on

$$\Pr\{K_j\} = \prod_{i=1}^{c_j} u_{i,j} \tag{2.33}$$

where c_j is the number of failed components in the mcs j, and $u_{i,j}$ is the individual unavailability of each of the c_j components in mcs K_j. Based on (2.21), $u_{i,j}$ is the ratio of the failure rate $\lambda_{i,j}$ of component i in mcs j to the sum of this same component failure rate $\lambda_{i,j}$ and repair rate $\mu_{i,j}$.

In order to complete the general discussion about availability calculation in systems with multiple components, let's consider some basic systems with commonly found relationships among the components. For large systems comprising components that are arranged in combinations of simpler well-known structures, it is usually possible to calculate availability characteristics of each of the structures separately and then combine the availability of all the structures in order to calculate the total system availability. The three basic commonly used cases are described next.

2.2.3.1 Series systems

If the system is not repairable – e.g., a circuit board with all its components soldered – the reliability can be evaluated based on what is commonly known as the "parts count" approach, in which the failure rate of the system is simply the sum of the failure rates of all the system components. That is,

$$\Lambda_{SYS} = \sum_{i=1}^{N_C} \lambda_i \tag{2.34}$$

where λ_i is the failure rate of the i-th component among the N_C forming the system and Λ_{SYS} is the total system failure rate. The MTTF for the system is, then, the inverse of Λ_{SYS}, and the reliability $R_{SYS}(t)$ of the system is

$$R_{SYS}(t) = e^{-\Lambda_{SYS} t} = \prod_{i=1}^{N_C} r_i(t) \tag{2.35}$$

where $r_i(t)$ is the reliability function of each of the components forming the system.

https://doi.org/10.1017/CBO9781139002998.003 Published online by Cambridge University Press

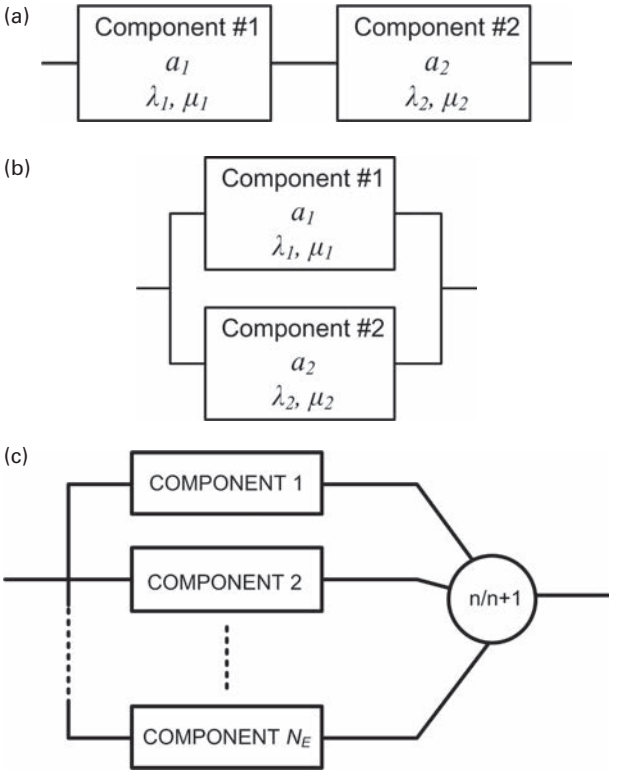

Figure 2.5 Availability success diagrams for (a) two series components, (b) two parallel components, and (c) $n + 1$ redundant components.

If the system is repairable and has two components, the availability success diagram is that in Figure 2.5(a). Since all components need to be operating for the system to be working, the availability of the two-component system is given by the steady-state probability of finding the Markov process represented by Figure 2.4 in state S_1, which is equal to the product of the availabilities of the two components A and B. For n components the availability is given by

$$A_{SYS} = \prod_{i=1}^{N_C} a_i \tag{2.36}$$

where a_i is the availability of each of the N_C components in the system. If all of these availabilities are close to 1 it is simple to show that

$$U_{a,SYS} \cong \sum_{i=1}^{N_C} u_i \tag{2.37}$$

which is analogous to (2.32) because in a series-connected system (from an availability perspective) each and all of the mcs are represented by a single component of all in the system. That is, $N_C = M_c$. The system's failure rate Λ_{SYS} is still given by (2.34). It is important to realize that in reality, in series systems there are no states representing the failure of more than one system component because it is assumed that failures are

https://doi.org/10.1017/CBO9781139002998.003 Published online by Cambridge University Press

independent of each other and they do not occur simultaneously, and because when one component fails the system ceases to operate, preventing further failures – i.e., S_4 in Figure 2.4 is not actually observed in a two-component series system. Based on this characteristic of series systems it can be found [1] that the system repair rate is

$$\mathrm{M}_{SYS} = \frac{\left(\sum_{i=1}^{N_C} \lambda_i\right)\left(\prod_{i=1}^{N_C} \mu_i\right)}{\left(\prod_{i=1}^{N_C} (\lambda_i + \mu_i)\right) - \left(\prod_{i=1}^{N_C} \mu_i\right)} \tag{2.38}$$

which for a system with highly available components – i.e., MDT<<MUT – can be approximated to

$$\mathrm{M}_{SYS} \cong \frac{\left(\sum_{i=1}^{N_C} \lambda_i\right)}{\left(\sum_{i=1}^{N_C} \frac{\lambda_i}{\mu_i}\right)} \tag{2.39}$$

2.2.3.2 Parallel systems

When system components are connected in parallel in an availability sense, all of the components need to fail in order for the system to fail. That is, there is only one mcs that includes all components in the system. Since there is only one mcs the expression in (2.32) is now exact so

$$U_{a,SYS} = \prod_{i=1}^{N_C} u_i \tag{2.40}$$

where u_i is the unavailability of each of the components. For a two-component system, the availability success diagram is that in Figure 2.5(b) and the unavailability is given by the steady-state probability of S_4 in Figure 2.4. As a dual case with respect to the series configuration the system repair rate is

$$\mathrm{M}_{SYS} = \sum_{i=1}^{N_C} \mu_i \tag{2.41}$$

and the system failure rate is

$$\Lambda_{SYS} = \frac{\left(\sum_{i=1}^{N_C} \mu_i\right)\left(\prod_{i=1}^{N_C} \lambda_i\right)}{\left(\prod_{i=1}^{N_C} (\lambda_i + \mu_i)\right) - \left(\prod_{i=1}^{N_C} \lambda_i\right)} \tag{2.42}$$

2.2.3.3 *n*+1 redundant systems

Consider a system that has a number of equal components that all serve the same function. Redundancy is a fault tolerance technique in which the system is equipped with more than the necessary minimum number of these equal components in order to

https://doi.org/10.1017/CBO9781139002998.003 Published online by Cambridge University Press

perform their required function adequately and keep the system operating. The most common type of redundancy is the n+1 system, in which the minimum number of components necessary to keep the system operating is n and one more component is added for redundancy. Its availability success diagram is represented in Figure 2.5(b). Based on the second definition of availability in Section 2.1, system availability is the probability of observing the system to be working. In n+1 redundant systems, this event – having the system working – is observed when all n+1 redundant components are operating normally or when n of the n+1 components are operating normally. Since there are ${}^{n+1}C_n$ ways in which n operating components can be selected from a group of n+1 components, the availability can be mathematically calculated as

$$A_{SYS} = {}^{n+1}C_n a^n u + {}^{n+1}C_{n+1} a^{n+1} \tag{2.43}$$

where a and u are the availability and unavailability, respectively, of the n+1 equal components in the n+1 redundant arrangement and where

$${}^{k}C_n = \binom{n}{k} = \frac{k!}{(n-k)!n!} \tag{2.44}$$

Hence,

$$A_{SYS} = (n+1)a^n u + a^{n+1} \tag{2.45}$$

When (2.45) is plotted (see Figure 2.6), it is possible to observe one important characteristic of n+1 redundant systems: as the minimum number of components n is increased, the system availability decreases; and for values of n large enough the system availability A_{SYS} is less than the individual component availability a. Figure 2.6

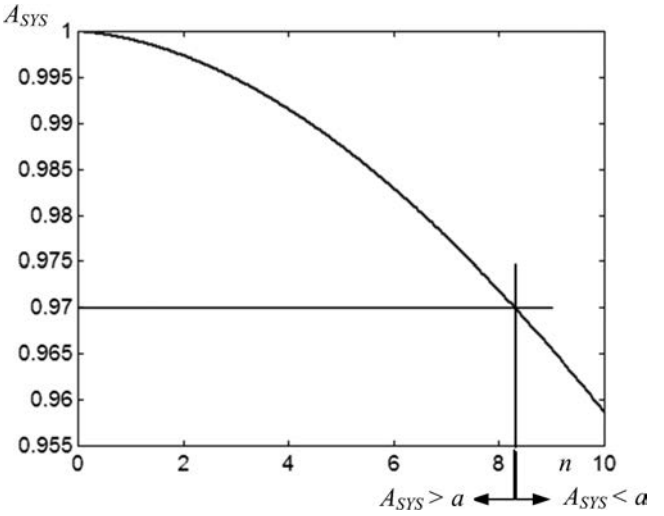

Figure 2.6 Availability of n + 1 redundant fuel cells versus the number of fuel cells necessary to operate the system.

https://doi.org/10.1017/CBO9781139002998.003 Published online by Cambridge University Press

exemplifies this property by considering fuel cells with $a = 0.97$. As this figure shows, for $n > 8$ the fuel cell arrangement availability is worse than that of a single fuel cell. Hence, redundancy is a fault tolerance technique that needs to be used with care, as increasing the number of components may compromise system availability instead of improving it. Finally, the failure and repair rates in an n+1 redundant arrangement are given by [1]

$$\Lambda_{SYS} = \frac{n\lambda^2(n+1)}{(n+1)\lambda + \mu} \tag{2.46}$$

and

$$\mathrm{M}_{SYS} = \frac{2({}^{n-1}\mathrm{C}_{n+1})\lambda^2\mu^n}{\sum_{i=0}^{n-1}\left({}^{i}\mathrm{C}_{n+1})\mu^i\lambda^{n+1-i}\right)} \tag{2.47}$$

respectively.

2.3 Common metrics and performance standards

The previous analyses imply that in order to calculate the availability of a system it is necessary to know the failure and repair rates of the components. Typical values for repair rates of a specific component may not be available because the rates may vary over a wide range of values that depend on the processes for maintenance, logistics, and storage of spare parts. For example, in the generic microgrid scheme in Figure 1.2, the power electronic interfaces between the sources and the distribution portion of the microgrid may be realized by various power electronic converter modules in an n+1 redundant configuration. If one of those modules fails, then the microgrid can still power the entire load unless another converter module fails. Thus, the microgrid is fully operational, but with increased chances of experiencing a failure until the failed component is repaired or replaced. Hence, it is important to identify how long it takes to replace the damaged converter module. The approach that leads to the shortest downtime is to have replacement parts on site, which facilitates rapidly replacing the damaged module within minutes. However, having spares on site implies some storage costs, particularly if the owner of the microgrid with the failed module needs to manage other microgrids. In these cases the maintenance manager may prefer to have fewer spares stored in a central warehouse, leading to longer downtimes for converter modules. Downtimes may be even longer (in the order of weeks) if the owner of the microgrid has no spare parts and needs to order them when a part fails or needs to wait for the damaged part to be sent to a manufacturing facility to be fixed and then for it to be sent back. That is, downtimes may extend from a few minutes to several weeks. Such a disparity usually leads to not having repair rates standardized or tabulated, as happens for failure rates.

https://doi.org/10.1017/CBO9781139002998.003 Published online by Cambridge University Press

Arguably, the most common source for failure rates of electronic and some electrical equipment is US Military Handbook 217F [2]. This handbook contains tables with data about the failure rates of most common electronic components and information about how to adjust the given base failure rate λ_b depending on the operational conditions of the component. That is, the failure rate of a component (λ) is in general given as

$$\lambda = \left(\prod_{i=1}^{N} \pi_i\right)\lambda_b \tag{2.48}$$

where π_i represents a series of factors that consider various relevant conditions for the component under evaluation that affect its base failure rate. Consider as an example the failure rate of a MOSFET used as a switch for a power electronic converter in a microgrid. Its failure rate is calculated based on [2]

$$\lambda = \pi_T \pi_A \pi_Q \pi_E \lambda_b \tag{2.49}$$

where λ_b is 0.012 failures for every million hours of operation. The failure-rate adjusting factors are:

- Temperature factor π_T: This factor is given in a table and depends on the junction operating temperature T_J. It can also be calculated based on the Arrhenius model, which is given by

$$\pi_T = e^{\frac{E_a}{k}\left(\frac{1}{T_R} - \frac{1}{T_J}\right)} \tag{2.50}$$

  where T_R is a reference temperature usually equal to 298 K (25 °C), T_J is the junction temperature in kelvin (K), k is the Boltzman constant ($k = 8.617\ 10^{-5}$ eV/K), and E_a is the failure activation energy, which in this case equals approximately 0.17 eV.
- Quality factor π_Q: This factor represents the quality of the component; generally other standards must be examined in order to obtain the complete and exact characteristics of each quality level. In the case of a MOSFET it can vary between 0.7 and 8.
- Application factor π_A. This factor allows the effect that different applications have on component reliability to be considered. For a MOSFET, π_A equals 2 when the rated power is between 2 and 5 W, 4 when the rated power is between 5 and 50 W, 8 when the rated power is between 50 and 250 W, and 10 for a rated power above 250 W.
- Environmental factor π_E. This factor considers the different stresses observed in varying environmental conditions, such as operation at a fixed location on the ground or moving on the ground, or operation in naval, airborne, or space applications. In the case of a MOSFET operating in a circuit at a fixed location on the ground this factor equals 6.

Due to their relatively low reliability, another interesting example is that of electrolytic aluminum capacitors. In these capacitors the failure rate is obtained from

https://doi.org/10.1017/CBO9781139002998.003 Published online by Cambridge University Press

$$\lambda = \pi_{CV}\pi_Q\pi_E\lambda_b \tag{2.51}$$

where the base failure rate λ_b is given in tables or calculated from

$$\lambda_b = 0.00254\left[\left(\frac{S_V}{0.5}\right)^3 + 1\right]e^{5.09\left(\frac{T_a}{358}\right)^5} \tag{2.52}$$

where T_a is the ambient temperature in K and S_V is the ratio of operating to rated voltages. For example, for T_a = 20 °C and S_V = 0.9, λ_b = 0.11 failures for every million hours of operation, i.e., about 10 times that of the MOSFET. This is not an unreasonable value because, typically, electrolytic capacitors are the least reliable components in a power electronics circuit. In this example of an electrolytic capacitor, the three factors affecting λ_b are:

1. Capacitance factor π_{CV}. This factor considers that failure rates increase as the capacitance increases because, among other reasons, of the more complex construction of the capacitor – typically aluminum electrolytic capacitors are built with a cylindrical shape that adds more layers in order to increase the capacitance; as the layers increase the chances of having a failure also increase. Mathematically, this factor can be calculated based on

$$\pi_{CV} = 0.34C^{0.18} \tag{2.53}$$

2. Quality factor π_Q. It represents the same effect on reliability as the one mentioned for the MOSFET. For a capacitor this factor is usually around 1, but in extreme cases it may take values as low as 0.03 and as high as 10.
3. Environmental factor π_E. The environmental factor has the same influence on the failure rate as what was mentioned for the MOSFET. In the case of a static application on the ground, π_E for a capacitor equals 2.

Notice that contrary to the repair rate, the failure rate is mostly dependent on hardware-related intrinsic and objective characteristics and conditions. Hence, failure characteristics typically allow for a more systematic assessment of the MUT (or MTTF if the object cannot be repaired) than of the MDT.

Other metrics that are often mentioned in order to evaluate power-supply reliability characteristics are those based on IEEE Standard 1366 [3]. This standard is typically applied to the distribution portions of electric power grids [3] and, hence, it is not well suited to consider the effect of assets found in LAPES, such as local distributed generation units or energy storage. Still, some works discussing availability in microgrids have nonetheless use availability metrics from IEEE 1366 for microgrids. However, this approach presents several issues when the goal is to analyze availability of a microgrid in a general sense. In order to better understand the limitations of the metrics contained in IEEE 1366 as applied to LAPES, let's present first some of the most relevant availability indices in [3]. Consider first the metrics applicable to sustained interruptions (those lasting more than five minutes):

https://doi.org/10.1017/CBO9781139002998.003 Published online by Cambridge University Press

– System average interruption frequency index (SAIFI)

$$\text{SAIFI} = \frac{\sum \text{total number of customers interrupted}}{\text{total number of customers served}} \tag{2.54}$$

That is, the numerator equals the sum of the "number of interrupted customers for each sustained interruption event during the reporting period" [3].

– System average interruption duration index (SAIDI)

$$\text{SAIDI} = \frac{\sum \text{customer interruption durations}}{\text{total number of customers served}} = \frac{\sum r_i N_i}{N_T} \tag{2.55}$$

where r_i is the "restoration time for each interruption event," N_i is the "number of interrupted customers for each sustained interruption event during the reporting period," and N_T is the "total number of customers served for the areas" under consideration [3].

– Customer average interruption duration index (CAIDI)

$$\text{CAIDI} = \frac{\sum r_i N_i}{\sum N_i} = \frac{\text{SAIDI}}{\text{SAIFI}} \tag{2.56}$$

– Average service availability Index (ASAI)

$$\text{ASAI} = \frac{N_T T_{H/Y} - \sum r_i N_i}{N_T T_{H/Y}} \tag{2.57}$$

where $T_{H/Y}$ is the number of hours in a year (8760 in a non-leap year and 8784 in a leap year). That is, the ASAI "represents the fraction of time that a customer has received power during the defined reporting period" [3].

– Customers experiencing multiple interruptions (CEMI_n)

$$\text{CEMI}_n = \frac{CN_{k>n}}{N_T} \tag{2.58}$$

where $CN_{k>n}$ is the total number of customers experiencing more than n sustained interruptions.

Other metrics in [3] are based on other evaluation parameters, such as a load's power consumption. These are:

– Average system interruption frequency index (ASIFI)

$$\text{ASIFI} = \frac{\sum L_i}{L_T} \tag{2.59}$$

where L_i is the connected load apparent power (in kVA) "interrupted for each interruption event" [3] and L_T is the total load apparent power (in kVA) served.

https://doi.org/10.1017/CBO9781139002998.003 Published online by Cambridge University Press

– Average system interruption duration index (ASIDI)

$$\text{ASIDI} = \frac{\sum r_i L_i}{L_T} \tag{2.60}$$

Finally, some metrics in [3] are specified for momentary interruptions. They are:

– Momentary average interruption frequency index (MAIFI)

$$\text{MAIFI} = \frac{\sum I_{Mi} N_{mi}}{N_T} \tag{2.61}$$

where I_{Mi} is the "number of momentary interruptions" and N_{mi} is the "number of interrupted customers for each momentary interruption event during the reporting period" [3].

– Momentary average interruption event frequency index (MAIFI_E)

$$\text{MAIFI}_E = \frac{\sum I_{ME} N_{mi}}{N_T} \tag{2.62}$$

where I_{ME} is the "number of momentary interruptions events" [3].

– Customers experiencing multiple sustained interruption and momentary interruption events (CEMSMI_n)

$$\text{CEMSMI}_n = \frac{CNT_{k>n}}{N_T} \tag{2.63}$$

where $CNT_{k>n}$ is the "total number of customers who have experienced more than n sustained interruptions and momentary interruption events during the reporting period." [3].

Although [3] provides a uniform framework to evaluate the availability of the distribution portion of power grids, it has some issues with use for LAPES. These issues are related to the purpose of [3]. This purpose can be summarized as providing a set of definitions that allows for uniformly reporting of distribution-side power outages among utilities operating in different settings, with dissimilar planning approaches, and with varying restoration practices and, in this way, allow for consistent comparison of distribution-side outage statistics both within a given electric utility and among various utilities. That is, [3] provides a uniform set of metrics and thus is not a method for availability calculation, as sometimes is stated. As a result, [3] is explicitly intended to be used *a posteriori* based on statistical data observed in a given period. Still, using Monte Carlo simulations it is possible to evaluate the expected availability behavior of a distribution portion of a grid. But the fact that [3] applies only to the distribution portion of grids presents the first challenge in its application to LAPES, because microgrids present a different technological platform, in which local distributed generation units, energy storage, and loads are integrated in a single system that may not be simple to divide in sections, as happens in power distribution portions of large conventional power grids. As a result, technical

https://doi.org/10.1017/CBO9781139002998.003 Published online by Cambridge University Press

inconsistencies appear when applying [3] metrics to microgrids, versus the conventional approach of applying the same indices to standard power grids. Moreover, the variety of approaches to developing microgrids – e.g., dc or ac power distribution voltages – leads to lack of uniformity in the metrics indications obtained when applying [3] to LAPES. For example, in microgrids it is possible to have a single load, in which case indices such as SAIFI or ASIFI do not provide consistent or valuable metrics. Another important aspect that limits the application of [3] to microgrids is the fact that in calculating the indices of [3], statistics are calculated excluding outages occurring in what is defined as a "major event day." That is, outages caused by natural disasters and other extreme events are not considered as part of the calculation of the metrics. However, one of the uses that has been identified for LAPES is precisely to improve power supply when extreme events happen. Therefore, although in most cases it is technically possible to use [3] to calculate availability metrics of microgrids' distribution portion, the results will most likely lack uniformity and their value may in most cases be limited. In reality, availability metrics in microgrids tend to be closer to those indicated for transmission portions of the grid in IEEE Standard 859 [4], which includes availability (expressed as service time/reporting period time) as one of the indices considered and which considers "major storm disasters" as one of its "exposure parameters."

There exist other well-known reliability and availability standards and metrics guides in addition to those just described. Two commonly used are Telcordia SR332 [5] and IEC 61709 [6]. Telcordia SR332 tends to be a guide similar to [2] in the sense that it also provides failure rate data for electronic components and indicates ways of adjusting base values depending on uses and operational conditions. The main differences are that [5] has been updated more recently than [2] and provides reliability estimations for civilian applications that are not as pessimistic as those obtained with [2]. That is, [2] tends to yield more conservative reliability values than [5]. In the case of [6], it is a standard with a broader use worldwide. However, it is more limited than [5] and [2], because [6] indicates how to obtain failure rates but does not provide failure rates data. In addition, it specifies reference conditions for obtaining failure rates and indicates how to adjust failure rates based on stress models.

2.4 Availability of LAPES

Arguably, development of modern LAPES has been driven by two main goals: interest in integrating renewable energy sources at a local level and search for approaches to improved power supply availability through ultra-available power systems. One of the main requirements of ultra-available systems is that they maintain full system operation when one or more failures occur. This characteristic is known as fault tolerance. A single point of failure is a portion of a system that causes the entire system to fail when it fails. Thus, fault-tolerant system design aims at eliminating single points of failure [7] [8]. Some common strategies to meet this goal [9] are:

https://doi.org/10.1017/CBO9781139002998.003 Published online by Cambridge University Press

- use of redundant components
- diverse implementation of the system functions
- distribution of critical system functions
- use of hot-swappable components

As it was explained above with respect to a LAPES, redundancy refers to a design in which the system has more than the minimum number of equal components required to deliver power. Diversity is a concept related to redundancy. However, while a redundant strategy involves using more equal components than the minimum required to perform a given function, diversity implies using additional but different system components than the minimum required to perform a given function. For example, having more microturbine units than those required to power the load refers to the use of redundancy, but adding microturbines to a cluster of fuel cells that can power the load alone refers to diversifying sources for a LAPES. Systems with distributed functions divide main system functions among various components. For example, in a LAPES with a distributed architecture, power distribution and conversion functions are spread among circuits and buses, and converters [10], respectively. Other important methods used to achieve fault tolerance are the provision of adequate means for online repairs by using modular hot-swappable components. In this way, availability is improved by reducing the MDT.

Implementation of fault-tolerant systems is not exempt from challenges. In general, system availability is increased at the expense of additional cost and complexity [11]. Hence, a balance has to be achieved in order to balance increased availability needs and reduced costs requirements. Fault detection and clearance become more complicated, especially in distributed systems. These challenges can be addressed. However, a realistic and balanced approach requires quantifying the analysis so that technological options can be assessed objectively. The rest of this chapter discusses how to quantify LAPES availability based on works referenced in [12] and [13]. Due to its simplicity and effectiveness, LAPES availability is evaluated using an mcs approach. Consider the general representation of a LAPES in Figure 1.2. A general Markov process graphical representation of this microgrid is shown in Figure 2.7. In this figure, each state represents an operational condition of a LAPES based on the operational condition of each of its components. As in Figure 2.2, 1 indicates a failed component, 0 an operating

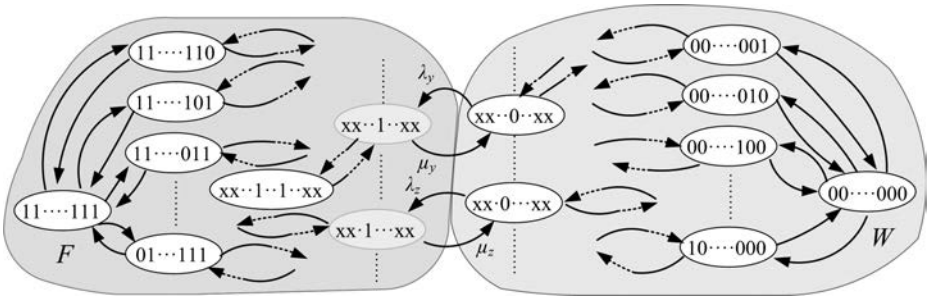

Figure 2.7 Markov process representation of a LAPES operational condition.

https://doi.org/10.1017/CBO9781139002998.003 Published online by Cambridge University Press

component, and x an unknown condition, which is not relevant to the discussion at hand. The set W includes all the states representing conditions in which the LAPES is operating, whereas the set F includes the states in which the LAPES is in a failed condition – i.e., it cannot power its entire load. The shaded states in F at the boundary with W imply that a repair to any of its failed components drives the system into an operational state. Hence, these shaded states are called minimal cut states (MCS) because each of them is associated with an mcs.

Based on (2.33), evaluation of a LAPES's availability using mcs requires calculating the unavailability of each of the mcs, which in turn requires knowing the unavailabilities of each of the relevant components and their interactions in an availability sense. Hence, the last part of this section discusses availability models and calculations for relevant system components of a microgrid and evaluates the effect that different circuit topologies for power electronic interfaces and various power architectures have on LAPES availability. This analysis is based on material presented primarily in [12] and [13]. Although specific assumptions are indicated at points of the discussion where they are relevant, some general assumptions considered in the analysis are:

- Failures are considered to be independent of each other. That is, failure of one component does not cause a failure in another component.
- For simplicity, it is assumed that the load is constant and known. Such a load can also be associated with the expected (average) value of a variable load. Nevertheless, this assumption is not required for the proposed models to be valid. Instantaneously uncertain loads could also be considered.
- Also for simplicity, it is assumed that the entire load of the LAPES is a critical load, so if any portion of the load is lost, then the LAPES is in a failed state. That is, the LAPES is operational when the whole load is powered. Still, the analysis can easily be applied to any particular distribution circuit in a LAPES. When only a particular distribution circuit is considered, then the calculated availability will apply to such circuit only and the implied assumption is that failed states are those that correspond to cases in which it is not possible to have the entire load connected to the distribution circuit under study powered.
- Yet another general assumption made in the analysis is that since stability study is out of the scope of this chapter and discussed later in this book, the microgrid under evaluation has been designed and engineered to ensure adequate stability.
- All local power generation units that are not powering loads are in hot standby. An example of hot standby is a diesel generator idling; although it is not providing electric power, the engine driving the electric generator is still running, but at no load other than that originating in its internal losses processes.

2.4.1 Availability of local power generation units

Availability of local generation units depends on two factors: availability of the generation unit itself – i.e., the hardware component for that distributed generation unit – and

https://doi.org/10.1017/CBO9781139002998.003 Published online by Cambridge University Press

availability of the energy source necessary for the operation of the power generation unit under analysis. Examples of the latter include wind, natural gas, or diesel fuel. In terms of energy sources, there are two types of power generation units: those that require a delivery of such an energy source, which is typically contained in a fuel, and those that can obtain or harvest energy locally, which is typically related to renewable energy sources, such as wind or solar radiation.

2.4.1.1 Power generation units that require delivery of their energy sources

In these cases energy is delivered to the LAPES through some external infrastructure. Since the LAPES's operation then becomes dependent on these infrastructures in order to receive energy for its sources, these infrastructures receive the name of lifelines. Energy can be provided though the lifelines and into the power generation units either through a continuous fuel-delivery process or a discontinuous delivery process.

Continuous fuel delivery process

As represented in Figure 2.8, in most LAPES this model for fuel delivery applies primarily to natural gas, which is delivered continuously, usually to on-site microturbines, internal combustion engines, or fuel cells with local reformers. Natural gas infrastructure is, then, the lifeline of the LAPES needing natural gas provision. From an availability perspective, the natural gas distribution system can be considered to be connected in series with each of these generation units, so the availability of the combination of the continuously delivered fuel and each power generation unit equals the product of each of their availabilities. Practical values for these availabilities, MUT, and MDT are presented in Table 2.2. For example, the availability of power supplied by the microturbine in Figure 2.8 is the product of the availability of the natural gas $(1 - u_f)$ supplied to the microturbine and the availability of the microturbine $(1 - u_{DG})$. Numerically, the availability is $(1–2.5\ 10^{-5})(1–0.006)$, which equals approximately 0.9939.

Discontinuous fuel delivery process

Discontinuous fuel delivery processes are associated with various LAPES sources. For example, one of the most common ways of powering microgrids is diesel engines that

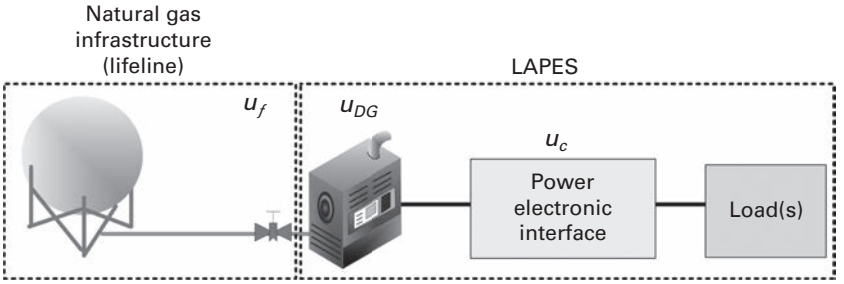

Figure 2.8 A simple LAPES powered by a microturbine, which is fueled through a natural gas pipeline.

https://doi.org/10.1017/CBO9781139002998.003 Published online by Cambridge University Press

Table 2.2 Availability-related parameters for key LAPES components. [13] [14]

Item and origin of the value	MUT (hours)	MDT (hours)	Availability *a*
Reciprocating engine	823	5	0.9939
Microturbine	8000	50	0.993 789
Natural gas supply	2 M	50	0.999 975
Diesel fuel supply		0.294	0.015
Converter		0.003	$3.33\ 10^{-4}$
$n + 1$ arrangement of seven converters		0.012	$3\ 10^{-6}$
PV generation system***	3636	14	0.996
Wind turbine ***	1900	80	0.9595
PEM fuel cell (performance degradation)	4679.75	156	0.967 742

*** Operational failure and repair rates considered for the times when sufficient energy is available as inputs to these power generation systems.

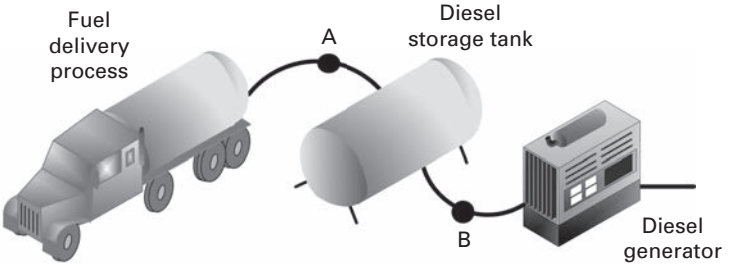

Figure 2.9 Representation of the fueling system for an internal combustion engine driving an electrical generator.

drive electric generators. Another example of a discontinuous fuel delivery process is a microturbine that receives energy from a bio-fuel. Yet another example is a fuel cell that receives hydrogen delivered in cylinders. In all these cases, fuel is delivered according to a defined process and stored locally in a tank from where the local power generation unit is fueled. Figure 2.9 shows a scheme of the infrastructure associated with the diesel generator in the first example. The terms "diesel supply" or "fuel supply" apply to the fuel flow at the generator's engine fuel intake indicated by point B in Figure 2.9, whereas "fuel delivery" refers to the end result of the logistical process involving oil extraction, diesel refining, distribution, selling, and transportation and actual delivery to the microgrid site, indicated by point A in Figure 2.9. If the diesel is flowing at point B, then the fuel supply system is considered to be *on*, or at a working state. If there is no flow of diesel at point B and the generator is commanded to run, then the fuel supply is considered to be at a failed state. Likewise, when the fuel system in Figure 2.9 is being refueled and diesel is flowing at point A, it is considered that the delivery process is at a working state. On the contrary, if no fuel is flowing at A because the system is waiting to be resupplied, then fuel delivery is considered to be at a failed state. Based on this model, fuel supply depends on the diesel delivery process, on the local energy storage (in the form of diesel contained in a tank with a capacity T_{TC}), and

https://doi.org/10.1017/CBO9781139002998.003 Published online by Cambridge University Press

on how this stored fuel is consumed, i.e., the operational regime. Three operational regimes can be usually considered for a power generation unit: continuous operation, cycling operation, and standby until a power grid outage occurs. This last operational regime is referred to in short as standby operation in the rest of this work, although "standby" does not imply that the genset is permanently in standby mode, but rather that it is in standby until a grid power outage occurs. Hence, based on the aforementioned assumptions, only the first operational mode is applicable to LAPES.

As a general case for reference, let's consider a diesel generator that requires periodic delivery of fuel, which is stored on-site in a tank. In most cases diesel is delivered using roads, so the transportation system becomes a lifeline of the LAPES. Since the LAPES load is assumed to be known and constant, the tank capacity provides a known autonomy indicated by T_{TC}. For variable loads characterized by a probability distribution function, the expected (average) value of such a probability distribution function can be considered for the calculations, because load changes will typically occur on a time scale much shorter – i.e., in the order of minutes – than the time scale for T_{TC} – i.e., in the order of hours or days. The fuel delivery process is characterized by a time t_d, which is the time that the fuel is delivered to the LAPES site; t_d is, then, a random variable that depends on a fuel-delivery probability density distribution function $f_d(t_d)$. Some of the possible forms for $f_d(t_d)$ are shown in Figure 2.10, which also shows three different instants that are important for the analysis: the initial time T_i when a fuel delivery may occur, the delivery time T_D when it is more likely that the fuel will have been delivered – e.g., due to a contract specifying the time for the delivery to happen – and the maximum time T_M, which is the last instant when it is possible to receive a fuel delivery. Among the possible forms for $f_d(t_d)$ shown in Figure 2.10, the exponential distribution may usually be a common first choice due to its simplicity and the analogous processes indicated in (2.10). However, the exponential distribution has some important issues. One of these issues is that its maximum occurs at $T_i = 0$ instead of at the defined delivery time T_D. Another problem is that it has no bound to the right because it is defined within a semi-infinite time interval $[T_i,\infty)$ – i.e., there are non-zero chances of having the fuel delivered in a time instant infinitely distant in the future. A uniform distribution would

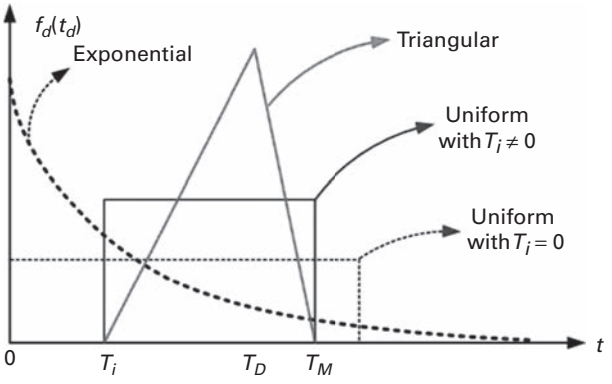

Figure 2.10 Various possible forms for the fuel-delivery pdf $f_d(t_d)$.

https://doi.org/10.1017/CBO9781139002998.003 Published online by Cambridge University Press

seem to be a somewhat more realistic representation of the fuel delivery process, particularly for the case in which $T_i \neq 0$, and it still would be simple to apply. However, a uniform distribution cannot represent the reality that fuel delivery will not occur with equal probability for any instant of time. Another possible fuel delivery distribution function, also shown in Figure 2.10, follows a triangular shape. Some of its advantages are that it is more realistic than the other two previously discussed distributions, yet at the same time it does not cause excessive calculation complexities. The triangular delivery distribution function represents a case in which there is a fuel contract that establishes a delivery time when fuel is due, indicated by T_D, but it also considers the real scenario that the fuel truck may arrive early, as indicated by the interval between T_i and T_D, or that problems along the delivery road may cause delays, so that the fuel delivery may still occur until a maximum possible time T_M. For simplicity, it is assumed that the probability density varies linearly, first increasing from T_i to T_D, when it reaches its maximum, and second decreasing from T_D to T_M. Mathematically, the triangular probability distribution function has the following form

$$f_d(t_d) = \begin{cases} 0, & 0 \leq t_d < Ti \\ \dfrac{2(t_d - T_i)}{(T_M - T_i)(T_D - T_i)}, & T_i \leq t_d \leq T_D \\ \dfrac{-2(t_d - T_M)}{(T_M - T_i)(T_M - T_D)}, & T_D \leq t_d \leq T_M \end{cases} \tag{2.64}$$

and its corresponding cumulative probability distribution function is

$$F_d(t_d) = \begin{cases} 0 & 0 \leq t < Ti \\ \dfrac{(t_d - T_i)^2}{(T_M - T_i)(T_D - T_i)} & T_i \leq t \leq T_D \\ F_d(T_D) + \dfrac{(-t_d^2 + 2T_M t_d + T_D^2 - 2T_M T_D)}{(T_M - T_i)(T_M - T_D)} & T_D \leq t \leq T_M \end{cases} \tag{2.65}$$

In (2.64), T_i and T_D are determined mostly from the negotiation process for a fuel delivery contract. On the other hand, T_M is determined mostly by transportation infrastructure performance and other factors leading to delivery delays. There are several ways of characterizing T_M. A simple approach is to assume that there is a probability P_{OD} that the fuel will be delivered some time between T_D and T_M. Hence,

$$F_d(T_D) = 1 - P_{OD} = \frac{T_D - T_i}{T_M - T_i} \tag{2.66}$$

from which T_M can be easily obtained. Entire fields of study, such as those related to logistics [15] or transportation sciences [16], have been dedicated to the analysis and characterization of P_{OD} or equivalent concepts. Some of these studies have been in the context of normal conditions [17] [18] and some others in the context of emergency conditions during disasters, which model both road network connectivity and delays [19]. Obviously a detailed discussion of P_{OD} is out of the scope of this work, but a simple, yet realistic approach for characterizing P_{OD} can be realized by first considering that

https://doi.org/10.1017/CBO9781139002998.003 Published online by Cambridge University Press

$$\Delta T_D = T_D - T_i \tag{2.67}$$

Even from an intuitive point of view it is simple to understand that if $\Delta T_D = 0$ then $P_{OD} = 1$, because if a delivery cannot occur before T_i and no practical realistic delivery can occur *exactly* at a specified time T_D, then it is certain that the delivery will occur after $T_D = T_i$. However, as ΔT_D increases, it is logical to expect that the chances of making the delivery within ΔT_D increase, meaning P_{OD} is reduced from 1. In the simple model considered here for discussion purposes, it is assumed that there is a delivery interval $\Delta T_{D,0}$ long enough to ensure that no deliveries will exceed T_D. Moreover, it is assumed that P_{OD} varies linearly from equaling 1 at $\Delta T_D = 0$ to equaling 0 at $\Delta T_D = \Delta T_{D,0}$. Thus,

$$P_{OD} = 1 - \frac{\Delta T_D}{\Delta T_{D,0}} \qquad \text{for } 0 \le \Delta T_D \le \Delta T_{D,0} \tag{2.68}$$

and

$$\Delta T_{D,0} = \frac{\Delta T_{D,ref}}{1 - P_{OD,ref}} \tag{2.69}$$

where $P_{OD,ref}$ is the probability of exceeding T_D that corresponds to a known interval $\Delta T_{D,ref}$. For example, assume that $T_D = 168$ hours, $T_i = 144$ hours, and $P_{OD} = 0.05$ when $\Delta T_D = 24$ hours. Then, $T_M = 169.26$ hours. Assume now that the time intervals between fuel delivery trucks are independent and identically distributed. It is also assumed that the truck replenishes the fuel tank instantaneously. Once a fuel delivery truck leaves, the next one arrives at the LAPES site at a random time t_d with an identical probability density function $f_d(t_d)$ as that for the previous truck. Since refueling occurs instantaneously, the generator's engine fuel supply from the diesel tank at the engine's fuel intake (point B in Figure 2.9) determines the unavailability of the fuel supply system. That is, when the diesel tank is empty, the fuel supply system is at a failed state. Since it is assumed that the load is constant and known (or for a variable load represented by its expected value over T_{TC}), the tank autonomy T_{TC} can be used in order to calculate the probability of emptying the fuel tank P_E, which equals the probability of failure for the generator. The probability of emptying the tank is the probability of having the fuel delivery truck arrive after a time T_{TC} has passed since the last refueling operation. Thus,

$$P_E = P\{t_d > T_{TC}\} = 1 - P_{E^*} = 1 - \int_{t_d=0}^{t_d=T_{TC}} f_d(t_d)dt_d \tag{2.70}$$

where P_{E^*} is the probability of not emptying the fuel tank. Obviously, choosing a T_{TC} long enough so that it exceeds T_M would ensure that $P_E = 0$, but problems may occur when P_{OD} increases from the originally planned values due to particular situations or events. For example, the chances of emptying the fuel tank may increase during extreme events because T_{TC} may be estimated for normal operating conditions based on values for P_{OD} and T_M that are much lower values than those that apply when a natural disaster

https://doi.org/10.1017/CBO9781139002998.003 Published online by Cambridge University Press

occurs. Obviously, T_{TC} will not be chosen to be shorter than T_D. Hence, it is assumed that T_{TC} falls in the interval $[T_D, T_M]$.

Based on [13], in order to find the fuel supply unavailability yielded by the described fuel supply model, assume that a very large number of refueling cycles have passed since the first one. It can be expected that in $100P_E$ percent of these cycles the fuel delivery truck arrived after T_{TC} with an expected fuel-supply downtime of MDT_f counted from the time when the generator stopped operating due to fuel starvation, which is the time T_{TC}. Obviously, with this same reasoning, it can be expected that in $100P_{E^*}$ percent of the cycles the fuel truck arrived before T_{TC} passed so that the generator does not fail due to fuel starvation. The ratio of the number of cycles when there is no generator failure due to engine fuel starvation to the number of cycles with fuel starvation is denoted as r and is calculated from

$$r = \frac{P_{E^*}}{P_E} \tag{2.71}$$

Over many refueling cycles it can be expected that r cycles lasting on average T_{E^*} are immediately followed by one refueling cycle lasting a time $T_{TC} + T_E$ in which the generator fails because it is out of fuel after running for T_{TC} hours. Since it is assumed that T_{TC} is selected within the interval $[T_D, T_M]$, MDT_f for a generator fuel supply model is

$$MDT_f = T_E = \frac{T_M - T_{TC}}{3} \tag{2.72}$$

so MUT_f equals

$$MUT_f = rT_{E^*} + T_{TC} \tag{2.73}$$

where for $f_d(t_d)$ given by (2.64) T_{E^*} is

$$T_{E^*} = \frac{(T_M - T_D)\int_{T_i}^{T_D} t(t - T_i)dt \; + \; (T_D - T_i)\int_{T_D}^{T_{TC}} t(T_M - t)dt}{(T_M - T_D)\int_{T_i}^{T_D} (t - T_i)dt \; + \; (T_D - T_i)\int_{T_D}^{T_{TC}} (T_M - t)dt} \tag{2.74}$$

Once MDT_f and MUT_f are known from (2.72) and (2.73), the fuel supply unavailability is

$$u_f = \frac{MDT_f}{MUT_f + MDT_f} \tag{2.75}$$

The failure and repair rates, λ_f and μ_f, respectively, equal the inverse of MUT_f and MDT_f, respectively. For example, consider a LAPES in which $T_D = T_{TC} = 72$ hours, $T_i = 48$

https://doi.org/10.1017/CBO9781139002998.003 Published online by Cambridge University Press

hours, and T_M = 82.28 hours because P_{OD} = 0.3. Then, MUT_f equals 221.3 hours, MDT_f equals 3.4 hours, and the fuel supply availability $a_f = 1 - u_f$ is 0.985.

2.4.1.2 Renewable energy sources

One of the advantages of renewable energy sources is that their operation is not dependent on the performance of a lifeline. However, their intermittent output complicates their application, particularly when the microgrid is operated disconnected from a main grid. It also complicates availability analysis because some of the premises and assumptions considered in the reliability analysis presented in this chapter are not applicable to failure situations associated with renewable energy sources, such as a failure of PV modules when there is not enough light to generate power. Another difference from the previous sources is that renewable energy sources may experience performance degradation; for example, when ice is accumulated on a wind turbine blade or when dust is deposited on a PV panel. These situations present nonpermanent conditions that would reduce the output of these sources but will not prevent them from delivering power to a load, and thus may not be considered failure conditions *per se*. Yet since output power is reduced, the chances of not being able to power the load increases, and thus availability decreases.

In order to provide some context for the analysis, consider first a case in which a LAPES has a PV array and that power output from the PV array and the load is sampled at regular intervals. In each of these intervals the power balance equation is given by

$$P_{stored}[t] = P_{PV}[t] - L[t] \tag{2.76}$$

where $P_{PV}[t]$ is the power supplied by the PV array and L is the load. If the available power from the PV array is greater than the demand of the load, $P_{PV}[t] > L[t]$, then the excess power is used to charge the batteries in the energy storage system associated with this renewable energy source. If $P_{PV}[t] < L[t]$, then the batteries provide the power difference between L and P_{PV} until such point in time that they become fully discharged. Thus, the presence of local energy storage is useful to manage the surplus or deficit instantaneous power. This is useful to reduce or even eliminate the variability observed from the perspective of the rest of the LAPES and can be designed using an economic-based analysis.

If the batteries are fully charged and cannot store additional energy, then power output from the PV array must be regulated so that $P_{PV}[t] = L[t]$. Alternatively, the surplus power can be injected into the electrical power grid if conditions permit. If the available power from the PV system is less than the requirements of the load, $P_{PV}[t] < L[t]$, and the batteries do not have sufficient energy storage capacity to provide the power deficit between the PV source and the (P_{PV}) and the load (L), then the combined system formed by the PV array and the batteries is considered to be in a failed state because the power demand of the load cannot be met. The focus of the following analysis is to evaluate the availability of the LAPES system comprised of the PV array and its associated batteries as a dispatchable stand-alone generation unit. Thus interaction with an electrical grid is not considered because such interaction would need to take into account a fourth

https://doi.org/10.1017/CBO9781139002998.003 Published online by Cambridge University Press

power-flow term: power flow from the LAPES to the utility grid. Although all power flow must be considered for each time interval, without loss of generality the explicit time dependence is dropped in the rest of this section to simplify the notation.

Performance degradation of PV modules due to aging or other factors, such as dust, can also be factored in (2.76) by considering that

$$P_{PV,d} = (1 - \delta)P_{PV,i} \tag{2.77}$$

where $P_{PV,i}$ is the ideal PV array power output and δ is a performance degradation factor. Reliability characteristics of PV modules can also be reflected in a similar way, by considering that a PV array's expected power output equals the availability of the PV array a_{PV} multiplied by $P_{PV,d}$

$$P_{PV} = a_{PV}P_{PV,d} \tag{2.78}$$

For PV systems, the performance degradation factor δ can take values between 0.002 and 0.007 per year [20], whereas a typical availability value for PV arrays is shown in Table 2.2. Wind power generation can be considered in the same way that PV power generation is. In terms of performance degradation, the factor δ may take various values depending on the degradation process. For icing δ may vary between 0.14 and 0.2 [21], whereas for dust accumulation δ may reach values up to 0.55 over a nine-month period in areas with high dust concentration and no rain [22]. Availability values for wind turbines are also indicated in Table 2.2.

The combined PV array/energy storage system is modeled using a Markov chain, shown in Figure 2.11, in which each state represents a state of charge or energy level of the energy storage system [23]. In Figure 2.11, each state transition, characterized by a probability p_i or p_{-i}, represents a charge or discharge process. For example, state 1 symbolizes the energy level of the storage system when it is fully discharged, and state N symbolizes its energy level when it is fully charged. If it is assumed that the energy storage devices have linear charge and discharge processes, the energy difference between any two adjacent states is Δ, so the power involved in such a process is Δ divided by the time step T_s between two consecutive steps in the Markov chain. Hence, p_{-i} generally represents the probability of a transition among states with an energy efflux of $i\Delta$ in T_s, and p_i represents the probability of a transition among states with an energy influx of $i\Delta$ in T_s, with i taking values from 1 to $N-1$. Then, the one-step transition probability matrix, P, associated with the Markov chain is

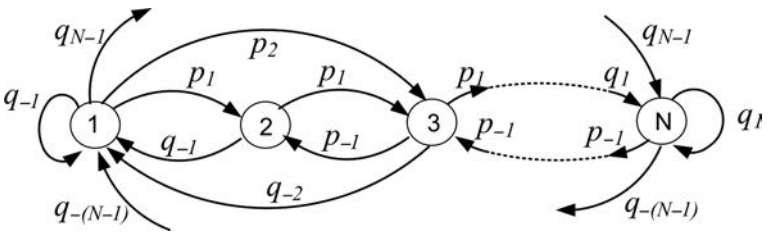

Figure 2.11 Markov chain for the PV array/energy storage system.

https://doi.org/10.1017/CBO9781139002998.003 Published online by Cambridge University Press

$$P = \begin{bmatrix} q_{-1} & p_1 & p_2 & p_3 & \cdots & & & \\ q_{-1} & 0 & p_1 & p_2 & \cdots & & & \\ q_{-2} & p_{-1} & 0 & p_1 & \cdots & & & \\ q_{-3} & p_{-2} & p_{-1} & 0 & \cdots & & & \\ \vdots & \vdots & \vdots & \vdots & \ddots & & & \\ & & & & & 0 & p_1 & q_2 \\ & & & & & p_{-1} & 0 & q_1 \\ & & & & & p_{-2} & p_{-1} & q_1 \end{bmatrix}_{N \times N} \tag{2.79}$$

where

$$q_{-1} = 1 - \sum_{i \in S} p_i \tag{2.80}$$

$$q_1 = 1 - \sum_{i \in S} p_{-i} \tag{2.81}$$

$$q_{-k} = 1 - \left(\sum_{i=1}^{k-1} p_{-i} + \sum_{i \in S} p_i \right) \tag{2.82}$$

$$q_k = 1 - \left(\sum_{i=1}^{k-1} p_i + \sum_{i \in S} p_{-i} \right) \tag{2.83}$$

The transition probability terms indicated by the terms q_k correspond to the particular cases when there is excess PV-generated power or a demand for energy beyond the battery capacity range. As with the other terms, a negative subscript corresponds to a battery discharge process and a positive subscript indicates a battery charge process.

Actual data from a particular location under study for each of both components P_{PV} and L in (2.76) can, then, be used as the basis of a Monte Carlo simulation in order to obtain probabilities of observing different values for P_B. That is, actual data is used to generate a discretized profile with a suitable distribution for each of both the load and the daytime incident PV power. These profiles are then used to generate multiple runs of random loads and incident PV power as part of a Monte Carlo process. In each run, the randomly generated value for L is subtracted from the randomly generated value for P_{PV}, yielding one value for P_B. A histogram can then be generated by accounting for the frequency at which each allowed value for P_B appears among the many Monte Carlo runs. In reality, (2.76) can be adjusted by separating loads profiles during daytime and nighttime in order to consider the fact that P_{PV} is always 0 during the night – a deterministic component of PV power generation. Then, the power balance equation becomes

$$P_B = P_{PV} - L_{day} - L_{night} \tag{2.84}$$

which implies that the night load is effectively shifted to daytime as a battery charging load for the PV array. Equation (2.84) can also be modified to consider wind generation in a hybrid system, as

https://doi.org/10.1017/CBO9781139002998.003 Published online by Cambridge University Press

$$P_B = (P_{PV} + P_{W,day} - L_{day}) + (P_{W,night} - L_{night}) \tag{2.85}$$

Once the histogram for P_B is known from the Monte Carlo runs, it can be used to obtain the values for the probabilities p_i and p_{-i} of each Markov chain transition in Figure 2.11. In turn, once the one-step transition probability matrix P is known, the limiting probabilities vector π can be found from [24]

$$\pi = \pi P \tag{2.86}$$

where each of the components in π represents the long-term steady-state probabilities that the energy storage system is at a certain energy state – e.g., π_1 represents the probability that energy storage is at state 1. Finally, unavailability u_{RW} of the system formed by the combination of the renewable sources and the energy storage devices can be calculated assuming that the load is not fully powered when energy storage is at state i and the load requires an energy of $i\Delta$ or more during the existing time T_s between two consecutive transitions of the Markov chain. Considering all possible transitions from all possible states for the considered time step T_s, the unavailability is

$$u_{RW} = \sum_{i \in \{1,N-1\}} \left(p_{-i} \sum_{j \le i} \pi_j \right) \tag{2.87}$$

Energy storage capacity affects unavailability through N and Δ, because the capacity is

$$C_{RW} = (N-1)\Delta \tag{2.88}$$

That is, by changing Δ it is possible to change P, which in turn modifies π, which results in a different value for u_{RW}.

Consider the following case as an example: A microgrid with a 100 kW load is operated in the city of Austin, Texas. In order to provide some generation overhead, assume that a PV array of 1.225 MW is used to power this LAPES, which implies an average power generation of 293.63 kW (variance = 68.2) from 7:00 am to 7:00 pm. Figure 2.12 shows the result of following the described method in order to calculate the availability for different energy storage capacities. If it is desired to achieve an availability of four nines (99.99%), then the equivalence of 0.9 days of energy storage is needed, which equals 1.16 MWh of battery energy storage (equal to 0.9 × 24 hrs. × 100 kW). If a five-nine availability (99.999%) is sought, then Figure 2.12 indicates that 1.15 days of equivalent energy storage capacity is needed, meaning a battery capacity of 2.7 MWh obtained for a time step T_S of one hour, and with Δ/T_S and N equal to 10 kW and 277, respectively. This example highlights two issues with renewable energy sources: the large energy storage capacity needed to achieve high availabilities and the large physical footprint needed to achieve the necessary power levels. One way of reducing the necessary energy storage capacity is to use diverse power sources. For example, when 225 kW of wind power generation is added, with an average daily generated power of 110.82 kW – so each group of wind or PV generators can sustain the load alone – the necessary energy storage to achieve an availability of five nines

https://doi.org/10.1017/CBO9781139002998.003 Published online by Cambridge University Press

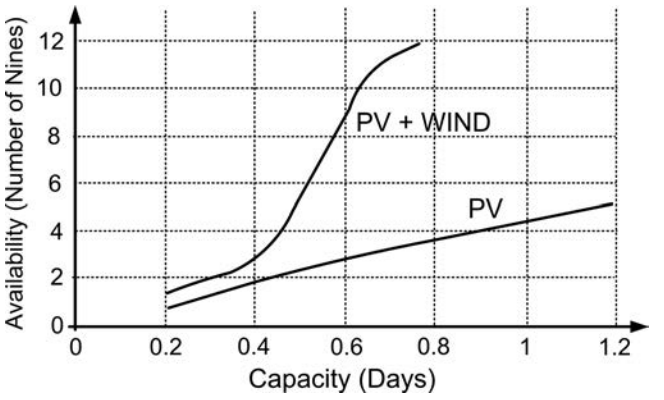

Figure 2.12 Availability obtained for varying energy storage capacities combined with a PV array or with a PV array and wind generators.

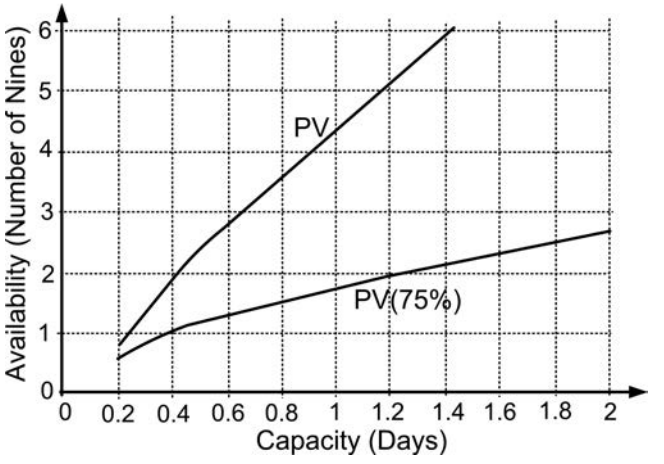

Figure. 2.13 Availability obtained for varying energy storage capacities combined with two PV arrays with different maximum power ratings.

decreases to about 0.5 days worth of load power, or 1.2 MWh. In terms of footprint, without wind generators the 1.225 MW PV array occupies an area of 6,125 m^2 in Austin because it is assumed that 200 W PV modules are used, which have a footprint of about 1 m^2 when they are installed with a tilt equal to the latitude of Austin of 30°. In order to reduce the footprint, it is possible to reduce the PV array capacity but availability is impacted. For example, a 25% reduction in the PV array capacity to 918.75 kW occupies 4,593.75 m^2, but for the same energy storage of about 2.7 MWh mentioned above, the availability is reduced from five nines to about two nines, or 99% (Figure 2.13).

Failure and repair rates for renewable energy sources can be obtained by assuming that Figure 2.11 represents the embedded Markov chain for a two-state Markov process in which state S_0 represents a failure condition for the renewable-energy power source plus energy storage and state S_1 represents the opposite situation. The equivalent Markov process is described, then, by

https://doi.org/10.1017/CBO9781139002998.003 Published online by Cambridge University Press

$$\dot{\pi}_{RW}^{T}(t) = \pi_{RW}^{T}(t)M = (\pi_{RW,W}(t) \;\; \pi_{RW,F}(t))\begin{pmatrix} -\lambda_{RW} & \lambda_{RW} \\ \mu_{RW} & -\mu_{RW} \end{pmatrix} \tag{2.89}$$

where the superscript index T represents a transpose operation, $\pi_{RW,W}(t)$ is the probability of having the system operating in state S_1 at time t, $\pi_{RW,F}(t)$ is the same probability for S_0, and M is the transition rate matrix for the two-state equivalent Markov process with failure rate λ_{RW} and repair rate μ_{RW}. The Markov chain and Markov process are related by [24]

$$M = \gamma(P - I) \tag{2.90}$$

where I is the identity matrix and γ is obtained from [24]

$$\gamma = \frac{1}{T_S}\frac{p_{11}}{1 - p_{11}} \tag{2.91}$$

where p_{11} is the element of P in row 1 and column 1; i.e., it equals q_{-1}. Hence, for the 100 kW load powered by the combination of a 1.225 MW PV array and batteries with a sufficient capacity to reach an availability of five nines, $\lambda_{RW} = 5.252\ 10^{-6}$ and $\mu_{RW} = 0.5252$, whereas for the hybrid system combining the same PV array, 225 kW of wind generation, and sufficient batteries to achieve an availability of five nines, $\lambda_{RW} = 8.189\ 10^{-6}$ and $\mu_{RW} = 0.8189$. When the target availability is two nines, $\lambda_{RW} = 5.2\ 10^{-3}$ and $\mu_{RW} = 0.512$ when only the PV array is present, and $\lambda_{RW} = 7.3\ 10^{-3}$ and $\mu_{RW} = 0.7219$ when the PV array is combined with wind energy.

2.4.2 Availability of power electronic interfaces

Power electronic interfaces (ac-dc rectifiers, dc-ac inverters, or dc-dc converters) impact the overall availability of a LAPES due to the individual availability as well as the way these devices are interconnected. This portion of Chapter 2 focuses on the former, the individual power converter, whereas the next section discusses the latter, interconnection of a plurality of power converters. The availability of each power electronic interface is given by (2.20) or (2.22). As it was mentioned, the MUT is mostly dependent on technical factors, such as design and manufacturing quality, and operational conditions. In comparison, the MDT is dependent on logistical, spares stocking, and maintenance policies and processes. The MDT is also dependent on system and power electronic interface design: a plug-and-play modular-based design tends to reduce the MDT by simplifying the process of replacing failed components.

One of the complex aspects of designing power electronic interfaces for LAPES intended for high availability operation are the tradeoffs between achieving high availability and, at the same time, meeting other important design objectives, such as reducing capital cost. Consider that a LAPES contains a critical load P_L. A failure condition exists when it is not possible to meet the entire power requirement of the load. Assume also that it is possible to express the cost for each ith power electronic interface as a function of the rated power (for example, the relationship can be linearly

https://doi.org/10.1017/CBO9781139002998.003 Published online by Cambridge University Press

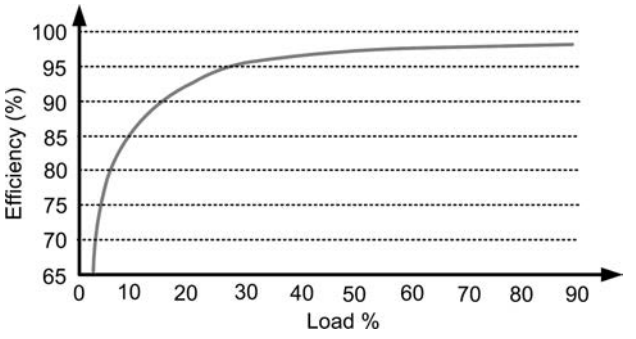

Figure 2.14 Typical efficiency profile for a power electronic interface.

proportional c_i/W), and that the availability of each power electronic interface module is a. If a central (unique module) power electronic interface is used, then the total capital cost is $\$P_L c$ and the power conversion system availability A equals a since there is only one converter. Now, consider that an n+1 redundant arrangement of similar power electronic modules are used in order to improve availability. The availability of the power conversion system is given by (2.45), which, as Figure 2.6 shows, decreases as n increases. It is also possible to find that the capital cost follows the same trend – decreasing as n increases – because the power p_m of each module equals P_L divided by n, so the capital cost is

$$C = c\frac{P_L}{n} \tag{2.92}$$

which decreases as n increases. A similar trade-off can be found with respect to the goal of achieving higher power efficiency. As Figure 2.14 exemplifies, the power efficiency of power electronic interfaces is typically lower with lower load. With no failed power interfaces modules, the power output of each of them is

$$p_o = \frac{P_L}{n+1} \tag{2.93}$$

so the ratio of the power output to the rated power is

$$\frac{p_o}{p_m} = \frac{n+1}{n} \tag{2.94}$$

which also decreases as n increases. Several approaches have been proposed to address issues related to the effects of reduced power efficiency at lighter loads. One is to improve the efficiency profile of power electronic interfaces to make it "flatter," using alternative control or circuit topologies design approaches. However, these solutions tend to add more control complexity or more components, which may lead to higher failure rates based on the parts-count calculation. Another approach that is commonly used in some applications, such as communication systems power plants, is to place modules that are not necessary to power the load in hot standby and to make the modules that are powering the load share it. However, this approach requires coordinating the

https://doi.org/10.1017/CBO9781139002998.003 Published online by Cambridge University Press

power output of each module so the load is equally shared. The simplest approach to achieve such coordination is to have a communication link among the power electronic interface modules, but this communication link may affect system availability by becoming a single point of failure. Although there are autonomous controllers that avoid the need for such a communication link, they add complexity and more parts, leading to a usually modest increase in the failure rate of each module.

2.4.3 Influence of power distribution architectures on availability

Differing wiring layouts and module topologies of power electronic interfaces affect how power distribution architectures influence system availability. Although the distribution portions of conventional power grids typically have a radial architecture, LAPES allow for alternative designs in order to improve certain operational parameters or characteristics (such as fault tolerance) due to their confined domain. Still, a radial configuration, such as the one in Figure 2.15, can be used, and in fact is typically the most common approach in microgrids. Two other possible power distribution architectures, ring configurations and ladder configurations, are shown in Figure 2.16 and Figure 2.17, respectively. Contrary to a radial power distribution architecture, in ring or ladder distribution architectures power can flow from local generators to loads through more than one path, and for this reason they are typically used in applications in which operation needs to be maintained even when at least one power path fails or is damaged (such as in microgrids for military bases). An analysis of the availability for these three power distribution architectures – radial, ring, and ladder – was presented in [25] following an mcs approach. This study concluded, as would be intuitively expected, that a radial power distribution architecture yields the lowest availability, while an equivalent well designed ladder power distribution architecture yields the highest availability. However, trade-offs between achieving low capital costs and high availability are observed in the design of the power distribution architecture, because although the ladder configuration achieves the highest availability of the three discussed approaches, it also tends to be the one with the highest capital cost – e.g., compare the wiring requirements and the number of circuit breakers in the three configurations – whereas the radial configuration tends to be the one with the lowest cost.

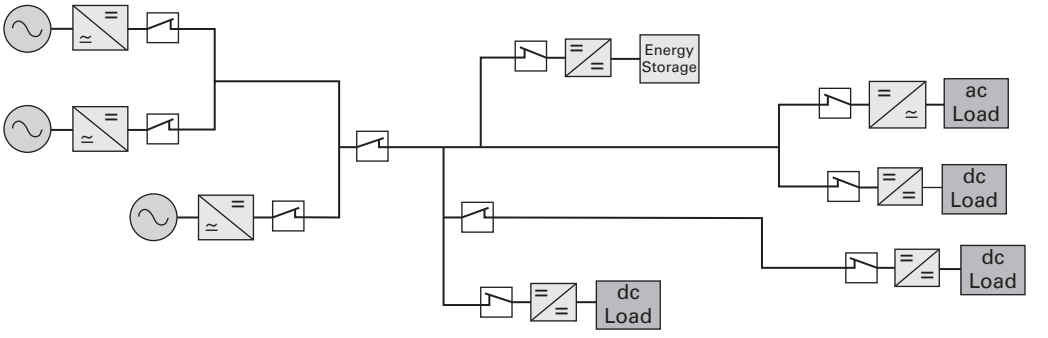

Figure 2.15 Radial power distribution architecture.

https://doi.org/10.1017/CBO9781139002998.003 Published online by Cambridge University Press

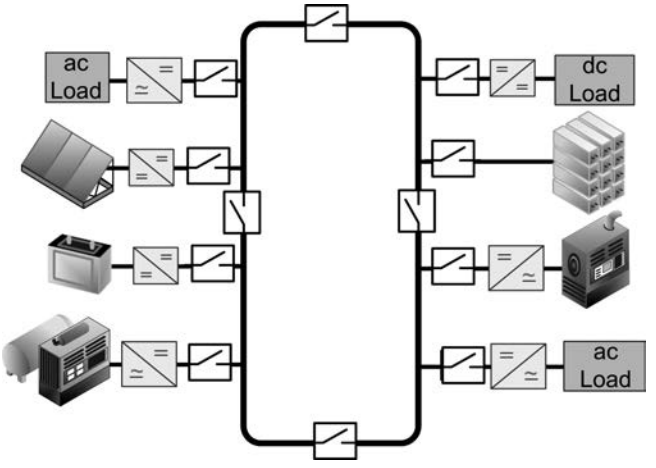

Figure 2.16 Ring power distribution architecture.

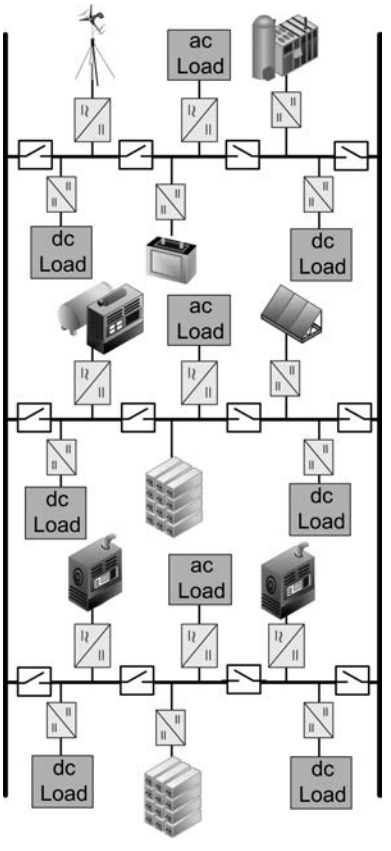

Figure 2.17 Ladder power distribution architecture.

https://doi.org/10.1017/CBO9781139002998.003 Published online by Cambridge University Press

Different circuit topology approaches for power electronic interfaces can also affect system availability through the influence that some circuit topologies have on the power distribution architecture configuration. As it is shown in Table 2.2, most distributed generation technologies have availabilities no better than about two nines, which is a considerably low baseline availability value that, in turn, makes it difficult to reach availabilities in the order of five nines or more as required by critical loads. Obviously, one solution is to have redundant local generation units of the same type, but this solution may increase the capital investment for a LAPES considerably, because many distributed generation technologies tend to have a relatively high cost per installed watt. Moreover, adding redundancy may not improve availability if the local power generation units are also depending on a lifeline with low availability. Another solution is to add energy storage devices connected to the microgrid main bus – a solution that will be explored in more detail in the next section. However, added energy storage may also have high capital costs. Yet another solution is to have diverse power sources of different technologies. In order to achieve ultrahigh availabilities the most probable suitable approach is to have a combination of these three different approaches: diversity and redundancy applied to the local power generation units and added energy storage. This combined approach has been already mentioned as a suitable solution when we mentioned that energy storage capacity in PV systems may be reduced by combining wind generation with solar-based generation. Hence, a cost-effective realization of a LAPES that combines these three strategies for high availability needs to consider how to integrate these diverse power sources (and in some cases energy storage) without adding significant capital cost from power electronic interfaces. But, as it was mentioned in the previous section, there exists a trade-off between achieving high availabilities and reducing the capital cost in power electronic interfaces. Finding a balanced approach to this trade-off between availability and cost may become more difficult when integrating diverse power sources. Thus, availability analysis cannot be decoupled from understanding the role that converter circuit topologies have on power distribution architecture designs and on LAPES availability.

A possible approach to studying the role of power electronic interface topologies in LAPES architecture and availability is discussed in [12]. In this study, an mcs approach is used in order to quantitatively calculate availability of microgrids considering three types of power electronic interfaces: a center single-input converter (SIC), represented in Figure 2.18, a redundant combination of a few modular SICs, and a redundant configuration of multiple-input converters (MICs), shown in Figure 2.19. Although MICs are discussed in detail in Chapter 4, in order to provide an understanding for the availability discussion provided here it is sufficient to explain that MICs are realized by dividing their homologous SICs into an output stage and an input stage and then multiplying the input stages that are connected to the same point to the common output stage. By sharing a common output stage MICs may reduce the capital cost of power electronic interfaces integrating diverse power sources with respect to the case of modular SICs. Moreover, as Figure 2.19 suggests, MICs create a meshed power distribution architecture that provides multiple power paths between sources and loads. The conclusion from the calculations in [12] is that power architectures with

https://doi.org/10.1017/CBO9781139002998.003 Published online by Cambridge University Press

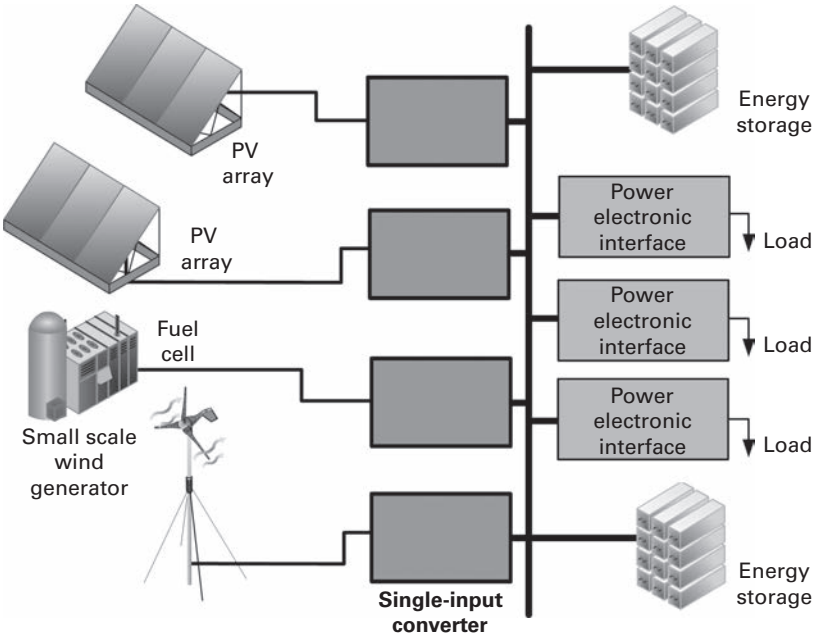

Figure 2.18 A LAPES with power distribution architecture with single-input converters interfacing individual local power generation units with the LAPES main bus.

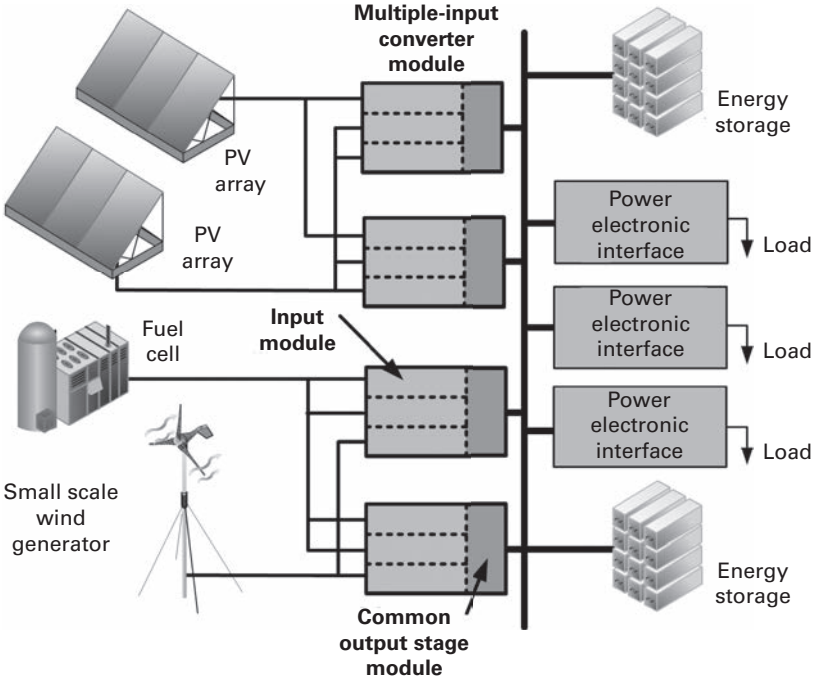

Figure 2.19 A LAPES with power distribution architecture with multiple-input converters interfacing local power generation units with the LAPES main bus.

https://doi.org/10.1017/CBO9781139002998.003 Published online by Cambridge University Press

MICs seem like a good compromise approach by providing the possibility of reducing capital cost in power electronic interfaces with respect to the case of modular SICs with only a marginal reduction in availability. Although less costly, configurations with center SICs have availabilities an order of magnitude worse than those calculated for modular SICs or MICs.

Power electronic circuits can also be used in power distribution nodes without necessarily interfacing sources or loads. In [26], multiple-input multiple-output bidirectional converters (MIMO-BCs), also called active power distribution nodes (APDNs), are proposed in order to address some issues that advanced power electronic distribution architectures present, such as those in Figures 2.16 and 2.17, in which circuit protection coordination with conventional devices, such as circuit breakers, is difficult to plan. In addition to providing a more flexible control of power flows, use of distribution-level converters can also address difficult fault current interruption in dc power distribution architectures. Moreover, when embedded distributed energy storage is placed in the MIMO-BCs, power availability can be enhanced because the embedded energy storage can provide energy backup to selected circuits. Furthermore, the conclusion in [26] is that although a higher parts count in MIMO-BCs leads to a lower availability than conventional approaches with circuit breakers, the use of embedded energy storage can overcome this lower availability in MIMO-BCs circuits, whereas the lower availability in circuit breakers that originates in alternative operational conditions, such as difficulties in interrupting dc fault currents, cannot be offset with any simple approach. Obviously, then cost becomes a concern as a configuration with MIMO-BCs and embedded energy storage has a higher hardware cost than a configuration with circuit breakers. However, the study in [26] also showed that the higher initial cost of MIMO-BCs with embedded energy storage could be compensated for, as the downtime costs in applications with critical loads is reduced as availability increases.

In order to assess the convenience in terms of availability of using power electronic interfaces over circuit breakers, [26] also presented an availability circuit breaker model that is shown in Figure 2.20. In this model, the circuit breaker has two parts: the interrupting device itself and the cable/conductor it is protecting. In Figure 2.20 λ_C is the failure rate of the conductor, ρ_{ID} is the interrupting device failure-to-open probability, μ_C is

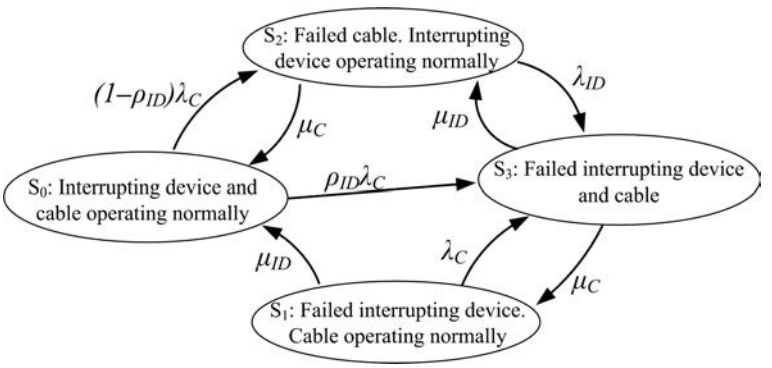

Figure 2.20 Availability model for a circuit breaker.

https://doi.org/10.1017/CBO9781139002998.003 Published online by Cambridge University Press

the conductor repair rate, λ_{ID} is the interrupting device failure rate, and μ_{ID} is the interrupting device repair rate. The interrupting device failure-to-open probability represents the fact that circuit breakers may also fail to isolate faults by not opening. Once all the parameters in Figure 2.20 are known, the availability of a circuit breaker can be calculated using the approach explained in Section 2.2.3 and detailed in [26], in which the availability is the long-term probability of being at state S_0.

2.4.4 Effect on availability of adding energy storage to a microgrid main bus

One effective way of improving availabilities of microgrids is to add energy storage – typically batteries – connected to the main bus or power distribution grid feeding the LAPES loads. The principle for improved availability through this strategy is simple: if there is a critical failure in any other portion of the system, by adding batteries connected at the loads' input the batteries can still power the load while the critical failure is repaired and the local power sources are able to power the load again. It is important to emphasize a significant difference of this energy storage system from source-level energy storage – e.g., stored diesel for an internal combustion engine generator or batteries for a PV system. The energy storage system discussed in this section and represented on the right of the microgrid power distribution grid in Figure 1.2 is connected on the load side of any power electronic interface used to integrate the local power generation units. Consider now Figure 2.7. From [1] and [27], the probability density function $f_{MG\mu}(t)$ associated with the probability of leaving the set F at time $t + dt$ after being in F from $t = 0$ is

$$f_{MG\mu}(t) = \mu_{FW} e^{-\mu_{FW} t} \tag{2.95}$$

where μ_{FW} is the sum of all the transition rates from F to W. Since, as Figure 2.7 shows, each of the minimal cut states at the boundary between F and W can be associated with an mcs, μ_{FW} can be calculated once the mcs are known, because repairing any of the components in an mcs drives the system from F to W. For example, as detailed in [13], the transition rate of an availability series arrangement of components from the MCSs into W is the sum of the repair rates of the components in the series configuration. Then, the probability of discharging the batteries while the system is in F since $t = 0$ is the probability of leaving F at a time longer than the battery backup time T_{BAT}. Hence,

$$P_{BD} = P\{t > T_{BAT}\} = 1 - \int_{\tau=0}^{\tau=T_{BAT}} f_{MG\mu}(\tau) d\tau = e^{-\mu_{FW} T_{BAT}} \tag{2.96}$$

The microgrid failure probability $P_{MGf}(t)$ is, then, the probability that the system failed at $t = 0$ and the batteries discharged to their minimum state of charge value. If it is assumed that the microgrid had been turned into operation a very long time in the past, then $P_{MGf}(t)$ equals the unavailability of the LAPES U_{MG} without distribution-level batteries, which is obtained, for example, from combining (2.32) and (2.33) – i.e., U_{MG} equals U_a in (2.32) if an mcs approach is used to calculate the microgrid availability up to the

https://doi.org/10.1017/CBO9781139002998.003 Published online by Cambridge University Press

output of the power electronic interfaces between sources and the microgrid power distribution grid. Thus, the microgrid unavailability with added batteries at the distribution level is

$$U_{MG,T} = U_{MG} e^{-\mu_{FW} T_{BAT}} \tag{2.97}$$

2.4.5 Additional considerations in terms of LAPES availability

The assumption that all local power generation units that are not powering loads are in hot standby (the fifth assumption in Section 2.4) is an important one in order to analyze LAPES availability. Although this assumption represents a real operational mode that is expected in most microgrids, it is possible that in some circumstances some generators are in "cold" standby: that is, they need to go through a start process in order to be able to take load. Hence, it is relevant to provide a method to assess availability with sources in standby.

Availability calculation of a power source in standby involves assuming that the system under study is not only the source in standby, but is actually the combination of a primary source and the standby source that starts to operate if the primary source fails. That is, the operation of the standby power source is dependent on the status of the primary source powering the load. Hence, since the system is composed of two components with an interdependent operation and each of these two components may be in a failed or a working condition, system availability can be modeled as the four-state Markov process represented in Figure 2.21. As it was defined before, in this Markov process each state is represented by two digits. The digit on the right identifies the status of the standby power generation source and the digit on the left characterizes the condition of the primary power source. A 1 is an indication of a failure and a 0 indicates a normal operating condition. The combined system formed by the primary source and the standby source is in a failed state when both of these sources are in a failed condition. From a calculation point of view, the unavailability of this combined system u_{SB} is given by [28]

$$u_{SB} = \frac{\lambda_{PS}(\lambda_{SBS} + \rho_{SBS}\mu_{PS})}{\mu_{PS}(\mu_{PS} + \mu_{SBS})} \tag{2.98}$$

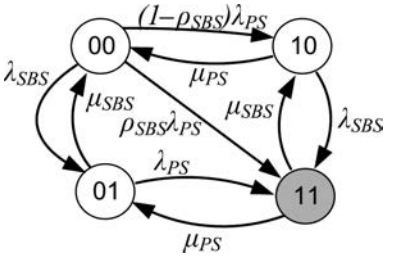

Figure 2.21 Markov availability model for a system with a primary source and a secondary standby generator.

https://doi.org/10.1017/CBO9781139002998.003 Published online by Cambridge University Press

where λ_{SBS} and μ_{SBS} are the failure and repair rates, respectively, of the series combination of the generator in standby and its lifeline, λ_{PS} and μ_{PS} are the failure and repair rates, respectively, of the primary source, and ρ_{SBS} is the failure-to-start probability for the standby power source. This failure-to-start probability represents the possibility that the generator in cold standby may experience a problem that prevents it from starting when it is called into service. Obviously, the higher the failure-to-start probability, the higher the unavailability is.

One of the main values of quantifying microgrid availability is performing objective comparisons among various technology options based on a lifetime cost evaluation that includes not only capital, financial, and operation and maintenance costs, but it also considers expected downtime cost – the cost associated with the loss of power to a given load. One approach to such evaluation is discussed in [29], in which risk assessment is used as the basic tool for technological assessment that includes microgrids. A detailed discussion of risk assessment is out of the scope of this work. However, it is relevant to mention that risk can be defined as the expected impact that a well-defined event may have on a system over an indicated period of time. Mathematically risk, R, is defined as

$$R = \Pr\{\text{Event}\}I \tag{2.99}$$

where I is the impact of the event. Impact is often considered as a monetary metric. In the case of downtime cost evaluations, the event could be that the system under study loses power for a given period of time due to some triggering event and the impact is the cost associated with having the load inoperable due to loss of power during the period of time being considered as part of the event definition. That is, the probability considered in (2.99) is associated with the unavailability of the evaluated LAPES and the risk R is the downtime cost considered as part of lifetime cost evaluations. It is important to mention that although risk analysis is an objective assessment tool, oftentimes planners may introduce subjective factors related to human psychology, culture, societies, history, and other factors. All of these factors may affect how humans perceive risk in terms of the probability and impact evaluation. For example, as discussed in [30] [31], before a natural disaster affects a given region, inhabitants of that area tend to perceive risk with a bias against the probability term – i.e., they see the event as less likely to occur or less likely that they will be impacted if it does occur – but after they are affected by a disaster they tend to focus their bias on the impact and tend to believe that the next time such an event happens their impact will be greater than what they expected it to be before the event happened.

2.5 Application of microgrids for resilient power supply during extreme events

One of the potential applications of microgrids introduced at the beginning of this chapter is improving the power supply when an extreme event happens.

https://doi.org/10.1017/CBO9781139002998.003 Published online by Cambridge University Press

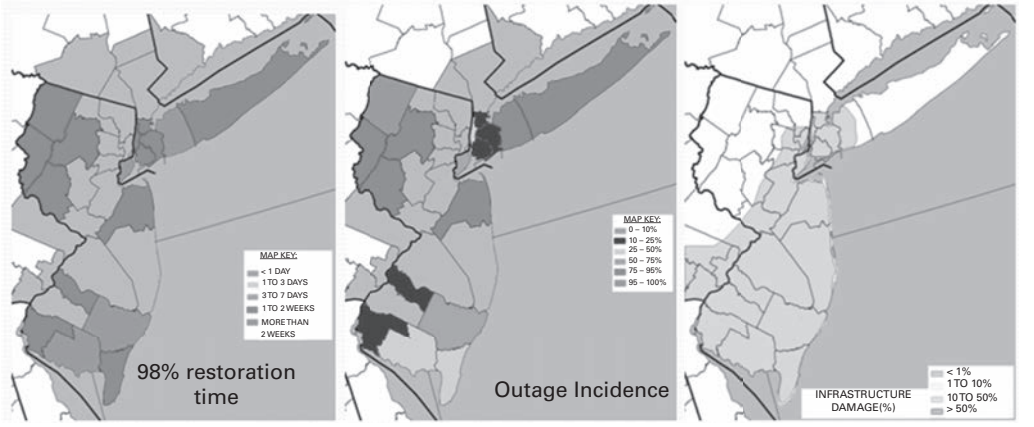

Figure 2.22 Power grid performance during Superstorm Sandy. From left to right: Time to restore service to 98% of the lost loads, peak percentage of customers that lost service during the storm, and damaged infrastructure percentage.

Figure 2.23 High Island, Texas, after Hurricane Ike.

The discussion in this chapter provides the tools to quantitatively assess potential advantages of microgrids over other solutions, such as powering a local area directly from a bulk power grid with or without support of a backup power solution, usually from diesel gensets. As Figure 2.22 illustrates, when a natural disaster (such as a hurricane or an earthquake) happens, it is possible to observe that conventional power grid outages are extensive and intense. Many times such power outages affect most or all customers in large areas for many days or even weeks. Yet such a severe loss of power is observed even in areas where there is relatively little damage, such as the ones in Figures 2.23 and 2.24. In fact, with most disasters severe power grid outages can be observed even when less than 1% of its components are damaged. Such relatively little damage is often

https://doi.org/10.1017/CBO9781139002998.003 Published online by Cambridge University Press

Figure 2.24 Union Beach, New Jersey, after Superstorm Sandy.

Figure 2.25 Crystal Beach, Texas, after Hurricane Ike.

observed in most of the area affected by a disaster, whereas severe damage, such as that in Figures 2.25 and 2.26, usually happens in less than 10% of the area affected by an extreme event. The fact that extensive and significant power outages happen with relatively few damaged power grid components suggests that the power grid is a very brittle system. This brittleness is caused by a number of factors and power grid characteristics, which include:

- predominantly centralized distribution architecture and control as seen by users
- passive transmission and distribution
- very extensive network (long paths and many components)

https://doi.org/10.1017/CBO9781139002998.003 Published online by Cambridge University Press

Figure 2.26 Area around Arahama Elementary School near Sendai, Japan.

- need for continuous balance of generation and demand
- difficulties in integrating meaningful levels of electric energy storage
- aging infrastructure

In recent years, and due to recent natural disasters, such as the 2011 earthquake and tsunami in Japan and 2012 Superstorm Sandy in the United States, there has been an increased focus on power grid performance characterized by the term "resilience." Yet in general there has not been a clear definition of what resilience is as it applies to power grids or how it could be measured. However, recently it has been proposed [32] to use availability as an analogous measure of power supply resiliency. Such an approach has also been suggested for communications systems [33]. When applied to the power supply, resilience R_e of an area with N_T customers or loads can be measured as

$$R_e = \frac{1}{N_T T} \sum_{i=1}^{N_T} T_{U,i} \tag{2.100}$$

where T is the period of time under consideration, $T_{U,i}$ is the part of T that a customer i is able to receive electric power – i.e., an "up" time – and $T_{D,i}$ is the remaining portion of T when a customer i may not able to receive electric power – i.e., a "down" time. The time T is chosen depending on which context resiliency is measured in. For example, it could be the interval from the time a disaster happens to the time that service is restored to all customers able to receive electric power. As is pointed out in [32], while $T_{U,i}$ is mostly dependent on hardware-related issues and how a power system is designed and built, $T_{D,i}$ is also dependent on "soft" factors, such as logistical, repair, spares-storing, and maintenance-management processes, and personnel training. Hence, LAPES and power systems in general can be considered human-cyber-physical systems, in which human-driven processes are also components of the system and analogous to electric power apparatus.

The metric in (2.100) is in agreement with the definition of resilience given both in US Presidential Power Directive 21 and in the report [34] prepared by the US National Academy of Sciences. The former defines resilience as "the ability to prepare for and adapt

https://doi.org/10.1017/CBO9781139002998.003 Published online by Cambridge University Press

to changing conditions and withstand and recover rapidly from disruptions" whereas the latter defines resiliency as "ability to prepare and plan for, recover from, and more successfully adapt to adverse events." That is, in (2.100) $T_{U,i}$ provides a measure of the withstanding characteristics, whereas $T_{D,i}$ provides a measure of recovery speed. Moreover, it is possible to find that the definition of resilience in (2.100) is not only related to availability metrics but it is specifically analogous to the ASAI in (2.57). The main reason the ASAI and R_e are analogous but not equivalent is that calculation of resilience through (2.100) does not require computing times based on an infinite number of extreme event cycles, whereas availability calculations, such as the ASAI, implicitly presume that times are calculated based on an infinite number of failure and repair cycles.

Section 2.4.1.1 showed that availability of microgrids can be affected by performance of lifelines. In general, the existence of a lifeline establishes a dependency relationship between a microgrid, or, in general, some dependent infrastructure and its lifeline. In [35], dependency between two infrastructures is defined in general as a "unidirectional relationship between two infrastructures through which the state of one infrastructure (lifeline) influences to the state of the other (dependent) infrastructure." As it was previously explained, in microgrids the dependency is established when local power generation sources require energy to be transferred from the lifeline to the microgrid's source. However, as discussed in [13] [32] [35], the concept of availability can be used in order to provide a measure for degree of dependency. Consider an ideal microgrid with perfectly available components, so that its availability depends only on its lifeline availability. If the microgrid has energy storage devices in order to maintain operation in case its lifeline experiences a loss of service, then the microgrid unavailability is given by (2.97). Ideally, if the total capacity of the energy storage device is infinite – that is, T_{BAT} in (2.97) is infinite (although here the stored energy may not necessarily be in batteries; energy could also be stored, for example, in diesel stored in a local tank) – then the microgrid unavailability is 0 regardless of the unavailability of the lifeline. This observation suggests that the amount of energy that is stored locally in order to achieve a target availability level could be used as a measure of degree of dependency D_D. That is, D_D could be defined as

$$D_D = -\frac{1}{\mu_D}\ln\left(\frac{U_t}{U_L}\right) \tag{2.101}$$

where U_L is the unavailability of the lifeline, U_t is a target availability – e.g., five nines in communication sites – and μ_D is the equivalent repair rate related to the inverse of the lifeline downtime measured at the connection point with the load or microgrid. Due to the analogous metrics between availability and resiliency, it is, then, also possible to define a measure for local resiliency R_L as

$$R_L = 1 - (1 - R_e)e^{-\mu_D T_S} \tag{2.102}$$

where T_S is the capacity of the locally stored energy at the load or microgrid measured with respect to the autonomy it provides during a lifeline loss of service and R_e is the

https://doi.org/10.1017/CBO9781139002998.003 Published online by Cambridge University Press

lifeline resiliency, which is analogous to $1 - U_L$. Hence, in an extreme ideal case, if a lifeline has a perfect ideal resiliency of 1, it is not possible to establish a dependency – i.e., D_D is 0 – and local resiliency is 1. Such observation can be explained based on the definition of dependency indicated above and the fact that a lifeline will not influence the performance of its dependent infrastructure (or load) if the lifeline always has the same "on" state that cannot be altered by any means. Moreover, both (2.101) and (2.102) show explicitly that the concepts of availability, resiliency, and dependency (or lifeline performance) are intrinsically related.

These concepts of resiliency can be considered from the perspective of a microgrid load, with the microgrid as its lifeline. Since there is no sufficient relevant data of microgrid operation during natural disasters, assume this is one of the cases of conventional power grids serving loads in a past notable disaster. Assume also that the load is an ideal communication site with a resiliency of 1 except for its lifeline – the power grid. As is standard for most communication networks, the target availability for such a site is five nines, but, as a reference, it could be assumed that the stored energy at the site allows for its operation for one day without power supplied from the electric grid. Since resiliency and availability are analogous concepts, a target resiliency of five nines is considered in this case study. Assume first that this site was located in Ascension Parish and suffered the effects of Hurricane Isaac in 2012, where a peak of about 56% of the electric loads lost power. At this location, where most of the power is distributed in aerial cables mounted on poles, it is possible to compute approximately $T = 18.2$ days, $T_D = 1.1$ days, $R_e = 0.96$, $D_D = 6.1$ days, and $R_L = 0.99$. In contrast, if the site was located in Manhattan, New York City, when Superstorm Sandy affected the area, causing about 40% of the loads to lose service, then the resiliency parameters are approximately $T = 18.75$ days, $T_D = 1.4$ days, $R_e = 0.92$, $D_D = 12.48$ days, and $R_L = 0.96$. When comparing these two cases, it is possible to conclude that the power grid in Manhattan seems to have been able to withstand the storm better than the power grid in Ascension Parish because in Manhattan a smaller portion of the load lost service. This observation is to be expected, because most of the power in Manhattan is distributed through buried conductors or cables in underground conduits. However, since buried cables take longer to repair than overhead infrastructure, service restoration in Ascension Parish was faster than in Manhattan, resulting in a more resilient power grid in Ascension Parish during Isaac than in Manhattan during Sandy. For this reason, the communications site's degree of dependence on the power grid was greater in Manhattan during Sandy than in Ascension Parish during Isaac.

There are several ways in which utilities try to improve resiliency during extreme events. Number of failures is reduced by implementing infrastructure-hardening programs, such as trimming trees, using reinforced poles, or burying cables and other components. However, burying infrastructure has a considerably high cost and may not be effective with earthquakes – and, as the previous example shows, although the failure rate is reduced, when a failure happens, repair times even in normal conditions are longer (i.e., there are longer down times). When an outage happens as a result of a disaster, some of the utility restoration strategies include the use of mobile transformers (Figure 2.27) and implementation of adhoc LAPES through the use of mobile

https://doi.org/10.1017/CBO9781139002998.003 Published online by Cambridge University Press

Figure 2.27 Mobile transformer and portable voltage regulators in the parking lot of the Peninsula Family Health Center in Far Rockaway, New York, after Superstorm Sandy.

Figure 2.28 A portable diesel genset connected on the power grid side of an apartment complex in Galveston, Texas, after Hurricane Ike.

gensets directly connected to the distribution grid (Figure 2.28). More recently, some other solutions that have been proposed are part of the new so-called smart grids that are discussed in more detail in Chapter 9. These smart-grid technologies, such as smart meters, allow for detecting outage locations faster, but this somewhat faster outage location detection will not avoid the need for electric utilities to eventually deploy crews

https://doi.org/10.1017/CBO9781139002998.003 Published online by Cambridge University Press

to repair the damage causing the outage. Another example of a smart grid–related technologies is to rely on grid-tied photovoltaic generation systems even during extensive power outages. However, as is detailed in Chapter 9, at the residential level these photovoltaic systems cannot operate during power outages, making them unsuitable for disaster conditions. Thus, most of these electric utility–based solutions tend to provide limited improvement to power grid resiliency during disasters, because they do not address the inherent issues present in conventional power grids that are listed above.

Since electric utilities' approaches to improving power supply resiliency during disasters are limited, electricity users have implemented alternative solutions. The most common and traditional approach is to use standby diesel generators. However, power grids' relatively low resiliency and standby gensets' relatively high failure-to-start probability sets an availability ceiling in normal conditions of about four nines, which is often insufficient for many critical loads, such as communication facilities. It can be anticipated that such an availability ceiling in normal conditions is much higher than the maximum resiliency value at the grid tie expected during extreme events, which could be at best on the order of one-nine. In order to reach the desired power resiliency level, the solution is for these loads to add energy storage – i.e., batteries – but such a solution is usually costly, because significant stored energy is usually needed. This context is where microgrids present an alternative solution with potential for achieving high resiliency levels.

Still, microgrid resiliency is not necessarily always high. Microgrids need to be well designed in order to achieve high resiliency levels. The main issues with an adequate microgrid design that is resilient to natural disasters are related primarily to local power sources' performance during such extreme events [13]. As has been discussed in this chapter, there are two types of local power sources: those that depend on a lifeline, and those that do not depend on a lifeline and that are usually based on renewable energy sources. The main issue affecting resiliency in disaster conditions for local power sources dependent on a lifeline is that the lifeline may be affected by the extreme event, such as the road in Figure 2.29. It is important to point

Figure 2.29 Louisiana Highway 23 south of New Orleans after Hurricane Isaac (2012).

https://doi.org/10.1017/CBO9781139002998.003 Published online by Cambridge University Press

out that lifelines are affected differently depending on the hazard being considered. For example, natural gas networks are usually affected little by hurricanes but are significantly affected by earthquakes. Thus, an effective design needs to consider the expected hazard at the microgrid location, and if possible a local power source technology should be chosen that relies on a lifeline that is affected the least by the potential hazard at the microgrid location. The issues affecting renewable energy sources are large footprints and partially stochastic power outputs. The approaches to addressing these issues in both types of local power sources are the same: diversify local power source technology and add energy storage to the microgrid. However, it is important to point out that there is a limit to how much energy storage can improve resiliency in LAPES powered by renewable energy sources only. This limit depends on excess generated power that can be used to recharge batteries. That is, although some added energy storage can address footprint and variable output issues of renewable energy sources without compromising resiliency, it is possible to find that adding energy storage capacity beyond a certain limit will not further improve resiliency because there will not be sufficient generated power in renewable energy sources to charge the energy storage devices above such a limit.

Obviously, the solutions explored here for enhanced power supply resiliency under the effects of extreme events, in particular from microgrids, are applicable to areas that may likely experience long power outages after a disaster but where the damage is minor. As it was mentioned above, damage assessments conducted after several recent natural disasters indicate that these areas with little damage but extensive power grid outages cover at least more than 90% of the areas affected by a natural disaster. For the rest of the areas, where damage is moderate to extreme, use of microgrids or other approaches may not be the most recommendable solution, because even when a microgrid can be designed to escape damage it is likely that an important portion of its load may be lost due to the disaster, and power-grid outage restoration by conventional means may be completed before most of the lost load is recovered.

When evaluating power technologies for enhanced power supply resiliency under the effects of an extreme event, it is also important to mention that the effects of disasters may last significantly longer than the event itself. Natural disaster effects can be divided into at least three phases: when the event is actually happening, the immediate aftermath, and the long-term aftermath. The events at the Fukushima #1 Nuclear Power Plant as a result of the March 11, 2011 earthquake and tsunami in Japan are an example of this characterization of events. The first phase occurred when the earthquake happened, triggering a tsunami that overcame the defenses at the nuclear power plant and damaged its cooling circuits. This first phase lasted for about two hours. The second phase lasted for a few days. During this second phase efforts at the nuclear power plant focused on preventing a nuclear accident and then, when the nuclear event finally occurred, containing its effects. The third phase is expected to last several years. In this phase, as a result of the Fukushima #1 Nuclear Power Plant event, Japan took all of its nuclear power plants off-line. This loss in

generation capacity added to loss of generation from several damaged conventional thermal power plants triggered the implementation of energy conservation measures, which under some extreme conditions may result in selectively rotating blackouts during days in which the load exceeds generation capacity. But another solution to the generation-capacity loss problem that could be implemented in combination with, or instead of, limiting demand is the use of distributed generation assets in order to limit the aggregated load seen by the conventional bulk-power generators in the main grid. That is, the benefit of a LAPES in terms of improving power supply resiliency extends months or years beyond the immediate need during and right after a natural disaster impacts a given area, and may even contribute to improved power supply resiliency outside of the local area served by the LAPES.

As with any new technology, there has been some reluctance in adopting microgrids extensively as a solution to improving power supply resiliency in all phases of an extreme event. One of the reasons for this reluctance observed in noncritical load applications originates in the higher cost of distributed generation technologies when compared with more traditional solutions. As summarized at the end of the previous section, these concerns about microgrids' costs may be objectively assessed by using risk analysis tools, as is detailed in [29], and by relying on the general economic analysis principles explained in Chapter 3. However, even when such an analysis favors the use of microgrids to achieve a highly resilient power supply during extreme events in critical load applications, such as in communication sites, widespread adoption of such new technologies in this type of critical application only occurs after extensive field trials. Obviously, this situation suggests a complex paradox in the technology adoption process: while due to the costs associated with distributed generation technologies it's expected that initial adopters of microgrids would be operators of critical loads, these same operators are reluctant to adopt such a technology until it has been extensively demonstrated in a practical setting – but to achieve such an extensive demonstration level, a broader utilization of microgrids is needed, which requires lower technology costs. One example of this paradox regarding such a reluctance to adopt new technology was observed at Verizon's Garden City central office in the aftermaths of Hurricane Irene in 2011 and Superstorm Sandy in 2012. This site is equipped with seven 200 kW fuel cells (Figure 2.30) that operate in parallel to the power grid serving this site. These fuel cells are intended to improve energy utilization in the building by reducing power consumption from the power grid. However, this site relies on conventional standby diesel gensets in order to power the site during outages in the power grid, and, obviously, during extreme events. That is, even when a suitable design combining energy storage and fuel cells can power this site autonomously, concerns about availability or resiliency – due to the fact that microgrids are not a technology that has been sufficiently tested to be used in critical load applications – led to the decision to still rely on conventional standby diesel gensets during the relatively long grid power outages that followed Hurricane Irene and Superstorm Sandy.

Figure 2.30 Seven fuel cells outside Verizon's Garden City central office.

Still, during recent disasters it has also been possible to document microgrid performance under the effect of extreme events. Even during Superstorm Sandy, a university campus and a US government facility were able to avoid losing power thanks to their natural gas–fueled distributed generation systems. Another example of demonstrated performance is a microgrid in the city of Sendai, Japan, which is operated by NTTFacilities. This microgrid was originally put into operation in 2008 as part of a project supported by the Japanese government agency NEDO, whose goal was to test the possibility of providing various electrical power quality levels through different circuits named dc, A, B1, B3, C, and "normal," depending on their expected power availability. The circuit with the lowest targeted availabilities was fed only from the bulk power grid tie, and the one with the highest availability was the dc circuit powered from a local energy center with a grid tie and supported by batteries (Figures 2.31 and 2.32). This local energy center was originally equipped with 50 kW of photovoltaic modules, two 350 kW natural gas generators, and a fuel cell, which had been removed by the time the earthquake struck on March 11, 2011. Thanks to its inland location and its hardened design the microgrid and surrounding area escaped the extreme damage observed in nearby coastal areas. Moreover, although the city's natural gas infrastructure was severely damaged, natural gas to the microgrid site was unaffected because the generators were fueled by a dedicated hardened natural gas pipeline from a storage center that also escaped damage from the tsunami because it was located inland. However, when the earthquake happened, voltage fluctuations in the public bulk power grid affected the operation of the natural gas engines, forcing them to go off-line. Efforts to bring them online a few hours after the earthquake struck were hampered by the batteries necessary to start the generators that were discharged. Finally, the two natural gas generators were brought back online about 21 hours after the earthquake happened.

https://doi.org/10.1017/CBO9781139002998.003 Published online by Cambridge University Press

Figure 2.31 Foreground: energy center in the Sendai microgrid. Notice the lack of significant damage compared to Figure 2.26 taken a few miles away.

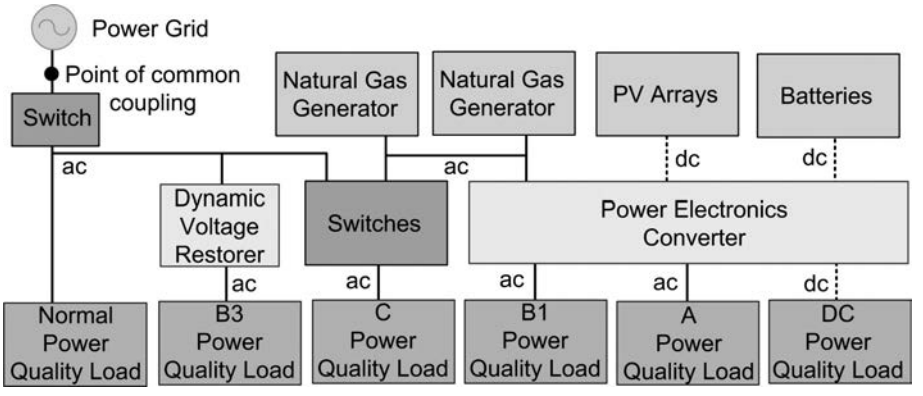

Figure 2.32 Block diagram of the microgrid in Sendai.

During those 21 hours, circuits B3 and C were not powered whereas circuits A and B1 were powered for the first 12 hours by the microgrid batteries. The dc circuit was kept powered the entire time by the microgrid batteries and the photovoltaic modules and never experienced loss of service. Once the natural gas generators were brought back online, all circuits except the one powered directly from the power grid were powered from the natural gas generators until power grid service was restored about 65 hours after the earthquake struck. At this time, service was restored to the normal quality service circuit.

https://doi.org/10.1017/CBO9781139002998.003 Published online by Cambridge University Press

2.6 References

[1] A. Villemeur, *Reliability, availability, maintainability, and safety assessment*. Volume **1**, *Methods and techniques*, West Sussex, Great Britain: John Wiley & Sons, 1992.

[2] U.S. Department of Defense, "Reliability Prediction of Electronic Equipment," MIL-HDBK-217, February 1995.

[3] "IEEE Guide for Electric Power Distribution Reliability Indices," IEEE Std 1366–2003 (Revision of IEEE Std 1366–2003), 2004.

[4] "IEEE Standard Terms for Reporting and Analyzing Outage Occurrences and Outage States of Electrical Transmission Facilities," IEEE Std 859–1987, 1988.

[5] Telcordia, "Reliability Prediction Procedure for Electronic Equipment," *Doc. Id. SR-332*, issue 3, January 2011.

[6] International Electrotechnical Commission (IEC), "Electric Components – Reliability – Reference Conditions for Failure Rates and Stress Models for Conversion," IEC Standard 61709, ed. 2, June 2011.

[7] R. V. White, "Fault Tolerance in Distributed Power Systems," *Proc. IV IEEE International Power Electronics Congress*, 1995, pp. 121–128.

[8] M. Di Giacomo, M. Martinez, J. Scott, and R. Luce, *A Fault-Tolerant Architecture for Supporting Large Scale Digital Libraries*, Number 38, Summer 2003, http://www.istl.org/03-summer/article3.html.

[9] A. Avizienis, "Toward Systematic Design of Fault-Tolerant Systems," *Computer*, issue 4, vol. **30**, April 1997, pp. 51–58.

[10] W. Tabisz, M. Jovanovic, and F. C. Lee, "Present and Future of Distributed Power Systems," *Proceedings APEC*, 1992, pp. 11–18.

[11] B. C. L. Lindemark, "The Impact of AC Power Line Disturbances on Telecommunications Rectifier Technologies and Powering Architectures," *Proc. INTELEC*, 1994, pp. 413–419.

[12] A. Kwasinski, "Quantitative Evaluation of DC Microgrids Availability: Effects of System Architecture and Converter Topology Design Choices," *IEEE Transactions on Power Electronics*, vol. **26**, no. 3, March 2011, pp. 835–851.

[13] A. Kwasinski, V. Krishnamurthy, J. Song, and R. Sharma, "Availability Evaluation of Microgrids for Resistant Power Supply During Natural Disasters," *IEEE Transactions on Smart Grid*, vol. **3**, no. 4, Dec. 2012, pp. 2007–2018.

[14] A. Kwasinski and P. T. Krein, "Multiple-Input DC-DC Converters to Enhance Local Availability in Grids Using Distributed Generation Resources," 2007 Applied Power Electronics Conference (APEC), Anaheim, CA, February 25–March 1, 2007, pp. 1657–1663.

[15] R. G. Kasilingam, *Logistics and Transportation, Design and Planning*, Dordrecht, The Netherlands, Kluwer Academic Publishers, 1998.

[16] M. G. H. Bell and C. Cassir, *Reliability of Transport Networks*, Baldock, Hertfordshire, Great Britain, Research Studies Press, 2000.

[17] J. Dong and H. S. Mahmassani, "Flow Breakdown and Travel Time Reliability," Transportation Research Record – Traffic Flow Theory, Characteristics, and Simulations Models TRR 2124, 2009, pp. 203–212.

[18] N. Wang, J-C. Lu, and P. Kvam, "Reliability Modeling in Spatially Distributed Logistics Systems." IEEE Transactions on Reliability, vol. 55, no. 3, September 2006, pp. 525–534.

[19] R. Nair and E. Miller-Hooks, "Evaluation of Relocation Strategies for Emergency Medical Service Vehicles," Transportation Research Record – Security; Emergencies; Management; and School Transportation TRR 2137, 2009, pp. 63–73.
[20] E. D. Dunlop, "Lifetime Performance of Crystalline Silicon PV Modules," *Proc. of 3rd World Conference on Photovoltaic Energy Conversion*, vol. **3**, 2003, pp. 2927–2930.
[21] W. J. Jasinski, S. C. Noe, M. S. Selig, and M. B. Bragg, "Wind Turbine Performance under Icing Conditions," *Transactions of the ASME, Journal of Solar Energy Engineering*, vol. **120**, Feb. 1998, pp. 60–65.
[22] M. G. Khalfallah and A. M. Koliub, "Effect of Dust on the Performance of Wind Turbines," *Desalination*, vol. **209**, issues 1–3, April 2007, pp. 209–220.
[23] J. Song, V. Krishnamurthy, A. Kwasinski, and R. Sharma, "Development of a Markov Chain Based Energy Storage Model for Power Supply Availability Assessment of Photovoltaic Generation Plants," *IEEE Transactions on Sustainable Energy*, in press.
[24] V. G. Kulkarni, *Modeling and Analysis of Stochastic Systems*, Second Edition, CRC Press, 2010.
[25] J. Song, M. C. Bozchalui, A. Kwasinski, and R. Sharma, "Microgrids Availability Evaluation Using a Markov Chain Energy Storage Model: A Comparison Study in System Architectures," *Proc. 2012 IEEE PES Transmission & Distribution Conference & Exposition*, Orlando, FL, May 7–10, 2012.
[26] M. Kim and A. Kwasinski, "A Storage Integrated Modular Power Electronic Interface for Higher Power Distribution Availability," *IEEE Transactions on Power Electronics*, in print.
[27] R. Billington and R. N. Allan, *Reliability Evaluation of Power Systems*, New York, Plenum Press, 1984.
[28] K. Yotsumoto, S. Muroyama, S. Matsumura, and H. Watanabe, "Design for a Highly Efficient Distributed Power Supply System Based on Reliability Analysis," *Proc. INTELEC* 1988, pp. 545–550.
[29] A, Kwasinski, "Technology Planning for Electric Power Supply in Critical Events Considering a Bulk Grid, Backup Power Plants, and Microgrids," *IEEE Systems Journal*, vol. **4**, no. 2, June 2010, pp. 167–178.
[30] L. Cameron and M. Shah, "Risk-Taking Behavior in the Wake of Natural Disasters," IZA Discussion Paper No. 6756, February 2011, 34 pages.
[31] G. Wachinger and O. Renn, "Risk Perception and Natural Hazards," CapHaz-Net WP3 Report, DIALOGIK Non-Profit Institute for Communication and Cooperative Research (available at: http://caphaz-net.org/outcomes-results/CapHaz-Net_WP3_Risk-Perception.pdf), Sept. 2010.
[32] A. Kwasinski, "Field Technical Surveys: An Essential Tool for Improving Critical Infrastructure and Lifeline Systems Resiliency to Disasters," in *Proc. IEEE 2014 Global Humanitarian Technology Conference*, San Jose, CA, October 2014.
[33] P. Trimintzios, Network Resilience and CIIP, "Measurement Frameworks and Metrics for Resilient Networks and Services: Challenges and Recommendations," European Network and Information Security Agency (ENISA), 2010.

[34] National Academy of Sciences, "Disaster Resilience: A National Imperative," Committee on Increasing National Resilience to Hazards and Disasters; Committee on Science, Engineering, and Public Policy; The National Academies, July 2012.
[35] A. Kwasinski, "Local Energy Storage as a Decoupling Mechanism for Interdependent Infrastructures," *Proc. 2011 IEEE International Systems Conference*, Montreal, QC, Canada, April 4–7, 2011, pp. 435–441.